


November 2014

New Generator Control Algorithms for Smart-Bladed Wind Turbines to Improve Power Capture in Below Rated Conditions

Bryce B. Aquino
University of Massachusetts Amherst

Follow this and additional works at: https://scholarworks.umass.edu/masters_theses_2

 Part of the [Acoustics, Dynamics, and Controls Commons](#), [Aerodynamics and Fluid Mechanics Commons](#), [Electro-Mechanical Systems Commons](#), and the [Energy Systems Commons](#)

Recommended Citation

Aquino, Bryce B., "New Generator Control Algorithms for Smart-Bladed Wind Turbines to Improve Power Capture in Below Rated Conditions" (2014). *Masters Theses*. 66.
<https://doi.org/10.7275/5576850> https://scholarworks.umass.edu/masters_theses_2/66

This Open Access Thesis is brought to you for free and open access by the Dissertations and Theses at ScholarWorks@UMass Amherst. It has been accepted for inclusion in Masters Theses by an authorized administrator of ScholarWorks@UMass Amherst. For more information, please contact scholarworks@library.umass.edu.

**NEW GENERATOR CONTROL ALGORITHMS FOR SMART-BLADED
WIND TURBINES TO IMPROVE POWER CAPTURE IN BELOW RATED
CONDITIONS**

A Thesis Presented

by

BRYCE BAUTISTA AQUINO

Submitted to the Graduate School of the
University of Massachusetts Amherst in partial fulfillment
of the requirements for the degree of

MASTER OF SCIENCE IN MECHANICAL ENGINEERING

September 2014

Mechanical Engineering

© Copyright Bryce Bautista Aquino 2014

All Rights Reserved

**NEW GENERATOR CONTROL ALGORITHMS FOR SMART-BLADED WIND
TURBINES TO IMPROVE POWER CAPTURE IN BELOW RATED CONDITIONS**

A Thesis Presented

by

BRYCE BAUTISTA AQUINO

Approved as to style and content by:

Matthew A. Lackner, Chair

Jon McGowan, Member

Yossi Chait, Member

Donald L. Fisher, Department Head
Mechanical and Industrial Engineering

ACKNOWLEDGEMENTS

I cannot express enough gratitude to Dr. Matthew A. Lackner for all of his support and guidance throughout this research. His mentorship and friendship throughout my time at the University of Massachusetts have been invaluable to me. The impact he has had on my life goes far past academia, and I am forever indebted to him for the opportunities he has given me.

I would also like to thank my committee members Professor Jon McGowan and Professor Yossi Chait for the insight and feedback during my research. This would not have been possible without their support.

A special thanks to Dr. Gerardo Blanco, Susan C. Belgrade, Evan Gaertner and Maura Coyle for editing my writing on such short notices. Your hard work is very much appreciated.

To all the graduate students in the Wind Energy Center, it has been a pleasure learning from you all throughout my graduate career. I will always treasure the countless hours we spent together in lab and all the late nights running simulations for our research. I wish you all the best of luck through your endeavors.

I am so grateful for my family, especially my mother, Pure, my late father, Jaime, and my cousins PJ, Phil and Marc, who have supported me throughout my years in Amherst, and for being there for me during hard times. And for my friends Ryan, Corn, Sy, PK, Lisa and Kevy for making my time in graduate school such a great experience. I value all the time we have spent together. Thank you for all the memories.

ABSTRACT

NEW GENERATOR CONTROL ALGORITHMS FOR SMART-BLADED WIND TURBINES TO IMPROVE POWER CAPTURE IN BELOW RATED CONDITIONS

September 2014

BRYCE BAUTISTA AQUINO

B.S.M.E., UNIVERSITY OF MASSACHUSETTS AMHERST

M.S.M.E., UNIVERSITY OF MASSACHUSETTS AMHERST

Directed by: Professor Matthew A. Lackner

With wind turbines growing in size, operation and maintenance have become a more important area of research with the goal of making wind energy more profitable. Wind turbine blades are subjected to intense fluctuating loads that can cause significant damage over time. The need for advanced methods of alleviating blade loads to extend the lifespan of wind turbines has become more important as worldwide initiatives have called for a push in renewable energy. An area of research whose goal is to reduce the fatigue damage is smart rotor control. Smart bladed wind turbines have the ability to sense aerodynamic loads and compute an actuator response to manipulate the aerodynamics of the wind turbine. The wind turbine model for this research is equipped with two different smart rotor devices. Independent pitch actuators for each blade and trailing edge flaps (TEFs) on the outer 70 to 90% of the blade span are used to modify aerodynamic loads. Individual Pitch Control (IPC) and Individual Flap Control (IFC) are designed to control these devices and are implemented on the NREL 5 MW wind turbine.

The consequences of smart rotor control lie in the wind turbine's power capture in below rated conditions. Manipulating aerodynamic loads on the blades cause the rotor to decelerate, which effectively decreases the rotor speed and power output by 1.5%. Standard Region 2 generator torque control laws do not take into consideration variations in rotor dynamics which occur from the smart rotor controllers. Additionally, this research explores new generator torque control algorithms that optimize power capture in below rated conditions.

FAST, an aeroelastic code for the simulation of wind turbines, is utilized to test the capability and efficacy of the controllers. Simulation results for the smart rotor controllers prove that they are successful in decreasing the standard deviation of blade loads by 26.3% in above rated conditions and 12.1% in below rated conditions. As expected, the average power capture decreases by 1.5%. The advanced generator torque controllers for Region 2 power capture have a maximum average power increase of 1.07% while still maintaining load reduction capabilities when coupled with smart rotor controllers. The results of this research show promise for optimizing wind turbine operation and increasing profitability.

TABLE OF CONTENTS

	Page
ACKNOWLEDGEMENTS.....	iv
ABSTRACT	v
LIST OF TABLES.....	x
LIST OF FIGURES	xii
CHAPTER	
1. INTRODUCTION	1
1.1 Literature Review	2
1.1.1 Standard Wind Turbine Control Overview	2
1.1.2 Advanced Wind Turbine Rotor Control Research	6
1.1.3 Advanced Generator Torque Control Research.....	8
1.2 Overview of Research.....	9
2. MODELING AND PROCEDURE.....	12
2.1 Wind Turbine Modeling	12
2.1.1 NREL 5MW Wind Turbine.....	12
2.1.2 Trailing Edge Flaps	13
2.2 WT_Perf.....	14
2.3 Turbsim	15
2.4 Aerodyn.....	15
2.5 FAST	17
3. ADVANCED CONTROL DESIGN	20

3.1 IPC and IFC Control Strategy	20
3.2 Proposed Generator Torque Control for Region 2	25
3.2.1 Gain Reduction of Generator Torque.....	25
3.2.2 Wind Speed Standard Deviation Torque Controller	25
3.2.3 Tip Speed Ratio Tracking Control	28
3.2.4 Power Production Sensitivity with Wind Speed Estimation Error	29
3.2.5 Smart Rotor Torque Regulator.....	31
3.2.6 Recalculating K Based on C_P for Varying Flap Deflection Angles.....	33
3.2.7 Linear Quadratic Regulation Control.....	37
4. RESULTS AND DISCUSSION.....	41
4.1 Smart Rotor Control Load Reduction Results	41
4.1.1 Below Rated Results	42
4.1.2 Above Rated Results	43
4.2 Power Loss	47
4.3 Advanced Generator Control Results.....	49
4.3.1 Generator Torque Gain Reduction Results	49
4.3.2 Wind Speed Standard Deviation Torque Controller Results	51
4.3.3 Tip Speed Ratio Tracking Controller Results	57
4.3.4 Power Production Results with Wind Speed Estimation Error	58
4.3.5 Smart Rotor Torque Regulation Results.....	61
4.3.6 Recalculating K based on C_P for Varying Flap Deflection Angle	62
4.3.7 Linear Quadratic Regulation Control.....	66
4.4 Overview of Results	69
5. CONCLUSIONS	70
6. FUTURE WORK.....	74
6.1 Smart Rotor Torque Regulator Control Refinement.....	74

6.2 Real Time K Calculations Based on TEF Deflection Angles.....	75
6.3 Offshore Analysis	76
BIBLIOGRAPHY.....	77

LIST OF TABLES

Table	Page
2.1 Design characteristics for the NREL 5MW wind turbine [4]	13
2.2 Aerodynamic blade properties for modified NREL 5 MW wind turbine with the addition of TEF [6].....	16
3.1 PID controller gains for IPC and IFC	23
3.2 Gain scheduled values for IPC and IFC controllers	23
3.3 State space matrices for approximate linearization of the turbine model with IFC activated	38
4.1 Load reduction potential for IFC, IPC and HYBRID controllers for above rated conditions	46
4.2 Average power output results in kilowatts for simulations while varying gain reduction and turbulence intensity	51
4.3 Percent change in average power output results for simulations while varying gain reduction and turbulence intensity, with optimums highlighted for each case	51
4.4 Power output for wind STD Controller	56
4.5 Percent power difference for wind STD Controller	56
4.6 Percent power loss for various error estimates	61

LIST OF FIGURES

Figure	Page
1.1 Power curve for NREL 5MW wind turbine with designated power regions [4].....	3
1.2 Example of a C_P vs. λ curve with designated optimal operating point	4
1.3 Schematic of Trailing Edge Flap (TEF) for wind turbine blades	7
2.1 C_P vs. λ (Tip Speed Ratio) mesh for varying flap deflection angle	14
2.2 Overview of FAST model for simulations	18
3.1 Schematic of control design for IPC and IFC controllers	24
3.2 Schematic of Wind Standard Deviation Torque Controller	28
3.3 Schematic of Tip Speed Ratio Tracking Controller	29
3.4 Wind Speed Error Estimation Controller	30
3.5 Coleman tilt angle and rotor azimuth angle for steady wind case	32
3.6 Schematic of Smart Rotor Torque Regulator (SRTR) controller	33
3.7 C_P vs Pitch Angle vs TSR mesh. An example of how power coefficient can vary with pitch angle [9]	34
3.8 Schematic for Optimal TEF CP Controller	36
3.9 Example of real time calculated K value for blades deflecting at different flap angles	37
3.10 Bode plot for frequency response of the linearized turbine model with inputs as Coleman angle and generator torque, and outputs generator power and flapwise root bending moment ..	39
4.1 Medium turbulent wind data to be used for simulations. Top graph has a mean wind speed of 8.5 m/s, while the bottom has a mean wind speed of 13.5 m/s	42
4.2 Comparison of IFC and SC flapwise root bending moments for blade 1 and IFC commands for each blade in below rated conditions	43
4.3 Comparison of root flapwise bending moment for SC, IPC and HYBRID controllers for above rated wind speeds	44
4.4 IPC and IFC commands for each blade in above rated conditions	45
4.5 Comparison of tower fore-aft bending moment for SC and HYBRID controllers	46
4.6 Reduction in generator power and rotor speed due to the addition of IFC controller in Region 2	47
4.7 Response of torque, power and rotor speed with ramping Coleman angle from minimum to maximum	48
4.8 Change in power output with K reduction for turbulence intensities of 0%, 20% and 30%	50

4.9 Simulation results for wind file with 10% turbulence intensity	53
4.10 Simulation results for wind file with 20% turbulence intensity	54
4.11 Simulation results for wind file with 30% turbulence intensity	55
4.12 Power output and generator torque commands from TSR tracking controller with IFC activated	58
4.13 Power output with wind speed error introduced to TSR tracking controller	59
4.14 Generator torque commands with wind speed error introduced to TSR tracking controller	60
4.15 New generator torque commands and power output for SRTR controller	62
4.16 Raw controller results for C_P calculation controller	63
4.17 Filtered results for C_P calculation controller	65
4.18 Step response of state space model	67
4.19 Step response with LQR controller for Q increased for power	68
4.20 Overview of Control Algorithm Results	69

NOMENCLATURE

C	Controllability matrix
C_D	Coefficient of Drag
C_p	Coefficient of Power
C_L	Coefficient of Lift
θ_{CM}	Coleman Angle
P	Coleman Matrix
M_y	Flapwise Root Bending Moment
τ_c	Generator Torque
P^{-1}	Inverse Coleman Matrix
IPC	Individual Pitch Control
IFC	Individual Flap Control
LQR	Linear Quadratic Regulator
LTI	Linear Time Invariant
LTV	Linear Time Variant
MIMO	Multiple Input Multiple Output
PID	Proportional-Integral-Derivative
Q	State weighting matrix
R	Control weighting matrix
ψ	Rotor Azimuth Angle
SRTR	Smart Rotor Torque Regulator
SC	Standard Control
λ	Tip Speed Ratio
TEF	Trailing Edge Flap

CHAPTER 1

INTRODUCTION

The worldwide green energy initiative has been one of the main catalysts for the increased focus on renewable energy, with United States aiming to produce upwards of 20% of its power generation from wind energy. With wind turbines growing in size to over 120 meter rotor diameter, it is vital to improve their performance and ensure reliable operations.

Wind turbines are subjected to fluctuating wind speeds, causing high frequency and high amplitude aerodynamic forces on the blades, which can lead to significant damage to the structure over time. One solution to this issue is reducing these fluctuating loads on the rotor, resulting in longer turbine lifespan, lower maintenance costs and more power production. *Smart rotor control* has been an active area of study with the goal of decreasing fluctuating loads on turbine blades by controlling actuators that then modify the aerodynamic. These concepts have been shown to effectively reduce blade root bending moments and high cycle fatigue in simulations.

Currently, most modern wind turbines are variable speed, i.e. capable of varying rotational speeds over a larger range of wind speeds and more efficiently capturing power. The control of the generator torque enables this variable speed operation, and so it is critical to control the generator torque in such a way that power output is maximized. Due to the constant fluctuations of wind, it is a challenge to optimally control generator torque.

Previous work has assumed that smart rotor control and generator torque control are two separate systems that are independent from one another. However, with the addition of smart rotor control, mitigation of blade loads has led to reduced power capture due to the actuators altering the aerodynamics of the rotor. In order to overcome this reduction in efficiency, new generator

torque control algorithms are needed to increase the power capture when smart rotor controllers are implemented.

This thesis investigates the load reduction capabilities of smart rotor control algorithms for a 5 MW variable speed wind turbine, while attempting to increase below rated power capture. Real time state space controllers for generator torque commands are tested in order to improve power capture, while trailing edge flaps (TEF) are utilized to reduce aerodynamically generated fatigue loads in below rated operation.

1.1 Literature Review

1.1.1 Standard Wind Turbine Control Overview

Significant work has been done to analyze and optimize the operation and control of wind turbines. Laks et al. illustrate in “Control of Wind Turbines: Past, Present and Future” [7], the standard control methods presently being used for variable speed wind turbines. The authors focus mainly on pitch and generator control in Regions 2 and 3 (defined below) of wind turbine power curves. The specific power curve for the NREL 5 MW wind turbine, which is used for this research, is seen in Figure 1.1.

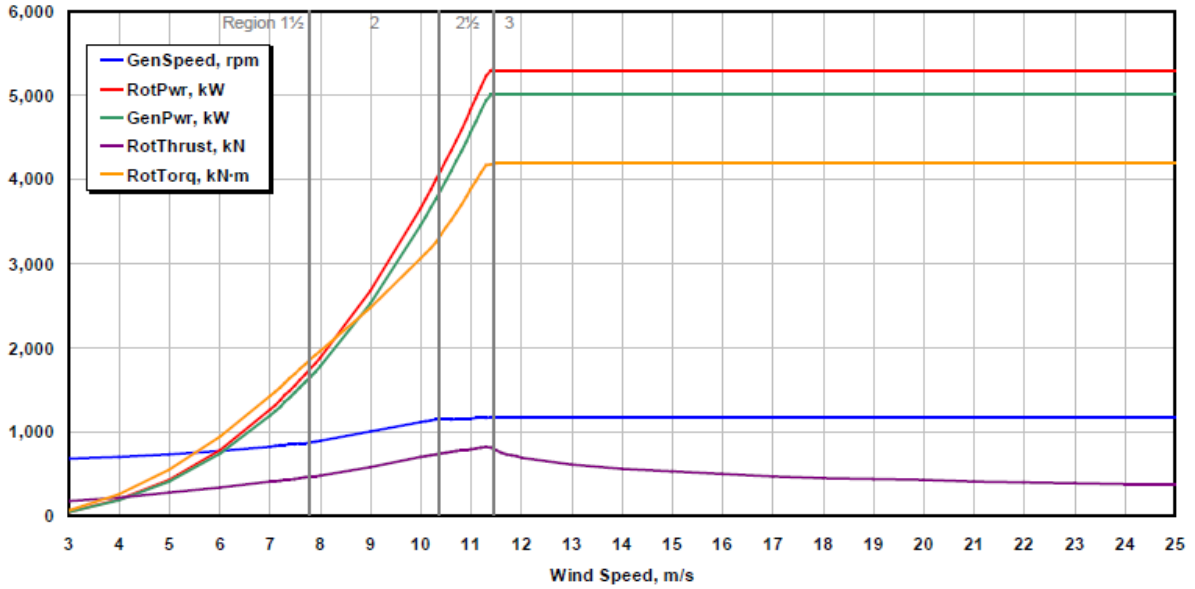


Figure 1.1: Power curve for NREL 5MW wind turbine with designated power regions [4]

Region 2 is defined as below rated operation. Blade pitch is held constant at its optimum value, such that the power coefficient is maximized. The tip speed ratio λ is the ratio of the speed of the blade tip divided by the wind speed shown in Equation 1.1 where u is wind

$$\lambda = \frac{BladeTipSpeed}{WindSpeed} = \frac{\omega R}{u} \quad (1.1)$$

speed, ω is rotor speed, and R is rotor radius. The goal in Region 2 is to preserve a constant λ value that corresponds to the optimal power coefficient for the rotor. That value, C_P , is the ratio of the rotor power to the power available in the wind, where P_{wind} and C_P are calculated as

$$P_{wind} = \frac{1}{2} \rho A u^3 \quad (1.2)$$

$$C_p = \frac{P}{P_{wind}} \quad (1.3)$$

where A represents rotor swept area and ρ is air density. Therefore, as seen in Figure 1.2, constant operation at the optimal λ results in the maximum power capture for the rotor.

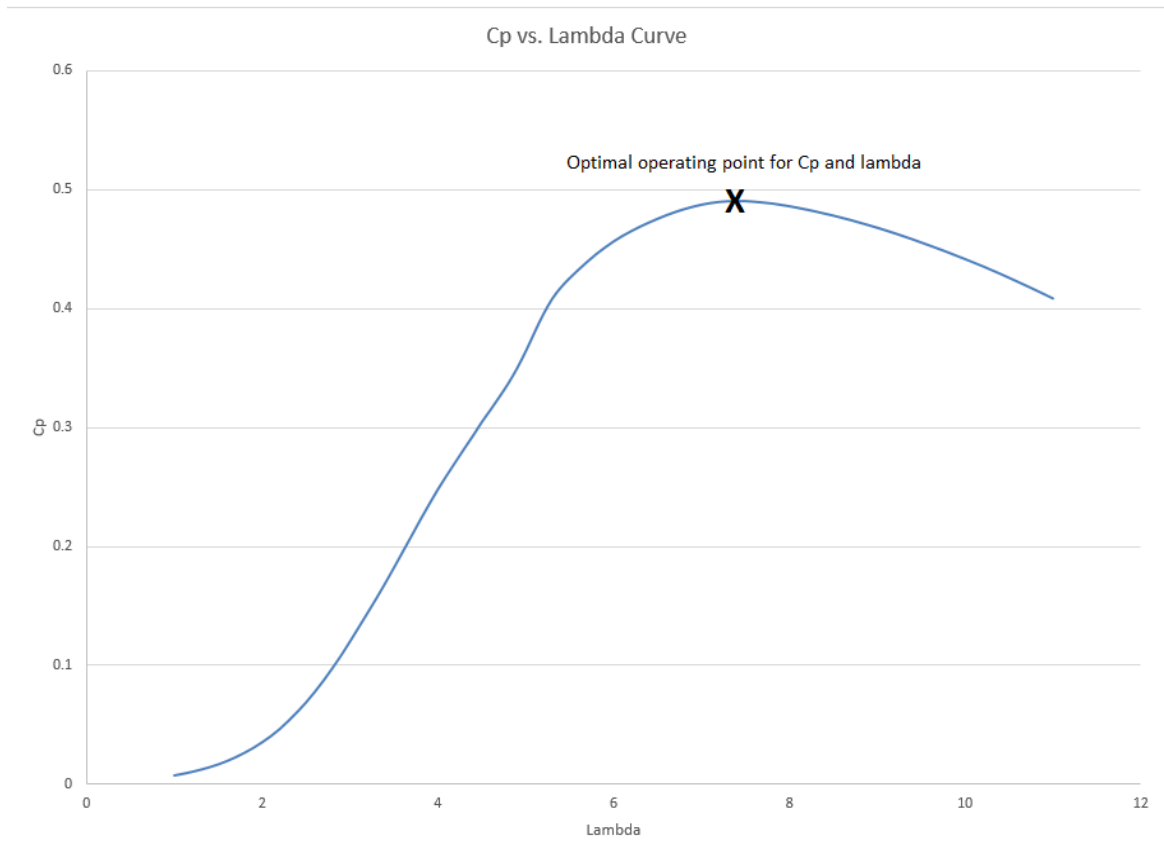


Figure 1.2: Example of a CP vs. λ curve with designated optimal operating point

In order to achieve a constant value of λ in Region 2 operation, the rotor must be operated with variable speed, so that ω may vary as u varies, preserving a constant value of λ . The generator is controlled in Region 2 to enable variable speed operation, and therefore to maximize power capture by matching the available aerodynamic torque with generator torque [5]. The generator torque τ is calculated by multiplying the square of the rotor speed, ω , by the generator torque gain K , as shown in the equation below.

$$\tau = K\omega^2 \quad (1.4)$$

K is calculated assuming ideal aerodynamic conditions for the turbine, which is rarely ever the case and is discussed further in this thesis. But in standard control, K is defined as

$$K = \frac{1}{2}\rho AR^3 \frac{C_{pmax}}{\lambda_*^3} \quad (1.5)$$

where ρ is air density, A is rotor area, and R is rotor radius.

Unlike Region 2, standard Region 3 controllers focus more on minimizing aerodynamic blade loading and producing constant power. Generator torque is held constant in this region. However, at these high wind speeds, aerodynamic loads and high rotor speed become an issue. In order to counteract these problems, the blades are pitched collectively towards feather, to regulate rotor speed as wind speed increases, preserving constant power operation. [6]

Laks et al. use a typical PID (Proportional Integral Derivative) control approach to design a pitch controller for Region 3 operation [8]. PID controllers are often selected over other types of

control, due their simplicity. They only require tune of the proportional, integral and derivative gains to produce desired system response characteristics. These gains correspond to present, past and future responses of the system based on the current rates of change. The overarching concept of these approaches is maximizing power output, while decreasing blade loads. However, due to the nonlinearities of the turbine modeling, there is a tradeoff when attempting to optimize the both objectives.

1.1.2 Advanced Wind Turbine Rotor Control Research

Smart rotor control defines a new class of rotors that can sense a disturbance, compute a reaction, and then actively control the aerodynamic loads in response to the disturbance. Advanced smart rotor control approaches such as Individual Pitch Control (IPC) have been previously researched by Bossanyi et al [3]. With wind turbine blades subjected to different loads due to wind shear and turbulence, controlling an individual pitch actuator for each blade can reduce the fatigue loading on individual blades.

Work done by Andersen has explored the effect of having Deformable Trailing Edge geometry (DTEG) on large scale wind turbine blades for load reduction [1]. By controlling the deformable edge of the blade, located on the outer span, coefficients of lift and drag can be changed with the goal of reducing structural vibrations and fatigue loading. Andersen explores different control approaches including a linear quadratic regulator (LQR) and PID controller. LQR control is a more complex control scheme, where in this case a state space model is created to approximate the relationship between the inputs and outputs. The outputs are weighted in importance by the controller algorithm. Due to the complexity of the model, which contains multiple state variables,

Andersen attempts many different combinations to achieve the most desirable results for the controller and finds that the algorithm complexities result in a similar outcome to a simple PID controller.

A study by Lackner explores the effect of combining both IPC and individual flap control (IFC) in a HYBRID approach to regulate blade loads in both above and below rated power conditions [6]. These trailing edge flaps (TEF) are located at the outer 70 to 90% span of the trailing edge of the blades, as seen in Figure 1.3. The flap is controlled by an actuator inside the blade, similar to mechanisms that are used for helicopter aerodynamics.

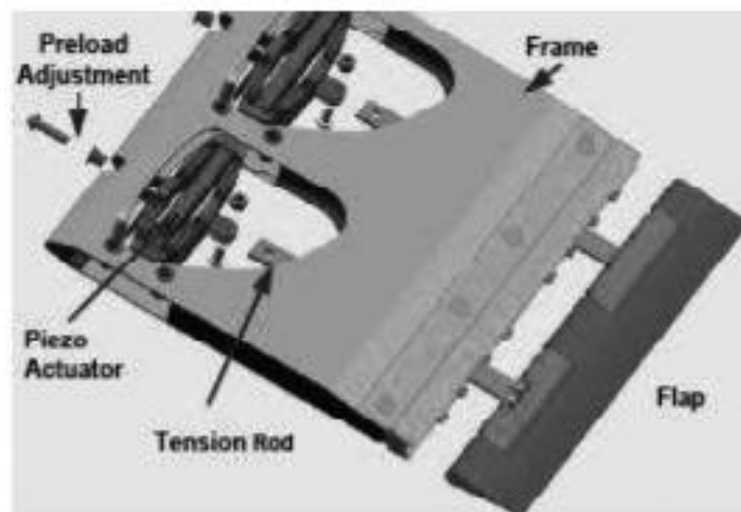


Figure 1.3: Schematic of Trailing Edge Flap (TEF) for wind turbine blades

The control approach is evaluated on the NREL 5MW wind turbine using an aeroelastic design code GH Bladed, developed by Garrad Hassan [6]. The IFC controller design created by Lackner is identical in approach to that of an IPC controller. Both use a feedback based PID controller regulated by blade root flapwise bending moment (M_y) for each blade and rotor azimuth angle (ψ). The experiment is simulated over a range of various wind speeds and achieves a

reduction in the blade fatigue loads of about 20% in both high and low amplitude loading, thereby decreasing the rapid fluctuations of loads on the turbine.

1.1.3 Advanced Generator Torque Control Research

As stated previously, Region 2 generator torque control has been an important area of research, because a significant portion of the turbine's operation takes place in below rated conditions. Ideally, a wind turbine should operate at a tip speed ratio λ that results in a maximum achievable power coefficient C_p . However, due to fluctuating wind speeds, it is difficult to obtain a constant optimal tip speed ratio λ , resulting in power loss in below rated conditions. Studies done by Balas, Pierce and Johnson have similar approaches to increasing Region 2 power capture for a variable speed turbine [2] [5] [9]. Pierce suggests an error estimation approach, where generator torque is controlled to increase and decrease rotor speed to match optimal TSR. By doing so, the amount of inertia transmitted to the rotor can be adjusted, which results in the ability to speed up or slow down the rotor. Controlling the turbine to operate closer to its optimal λ allows for more ideal operating conditions, resulting in improvement in power capture.

A different approach taken by Johnson et al. suggests that decreasing the generator torque gain produces better efficiency compared to the theoretically optimal value of the gain [5]. Because the gain K , which is in Equation 1.5 above, is mainly dependent on λ and therefore wind speed, it is a cubic function of wind speed. Due to turbulence, the wind speed constantly fluctuates while the rotor attempts to adjust to match its speed. By lowering K , inertia is transmitted to the rotor shaft, which help it to match the instantaneous change in wind speed due to turbulence. Therefore

the turbine operates at a more ideal λ . Through simulations, Johnson was able to achieve a Region 2 power increase of about 1% by decreasing K anywhere between 1-20%.

An alternative approach taken by Stol is attempting to increase power capture, while taking into the IPC behavior into consideration during control design. By linearizing a wind turbine model in SymDyn, an aeroelastic code used for wind turbine research, optimal set points are found for the states of wind speed, generator torque, blade pitch angle, and rotor speed. With this knowledge, a composite pitch plus torque controller is designed based on the error estimation of the set points calculated by a feedback loop [10]. An LQR control method is implemented with the error estimated from the state variables, while varying the weighting of the controller outputs, blade root bending moment and generator power. It is found that the presence of IPC affects the dynamics of the rotor and causes the power output to drop by 1% while decreasing the root bending moment by about 24% in amplitude. Conversely, without the presence of IPC, the composite torque controller is able to increase generator power by 1% compared to standard control. The results by Stol demonstrate the tradeoff between load reduction and efficiency due to the presence of smart rotor control.

1.2 Overview of Research

As stated previously, the focus of this research is to reduce fatigue damage by alleviating fluctuating loads on the rotor through smart rotor control, while increasing energy capture in below rated conditions. Similar approaches that have proven to be successful are implemented in the design and analysis of the turbine model. New methodologies are also explored with a goal of

creating an innovative strategy for increasing power capture with the presence of smart rotor control.

The modeling and simulation for this research is performed in FAST, an open source computer aided engineering tool for horizontal axis wind turbines developed by Jason Jonkman at the National Renewable Energy Laboratory (NREL). The baseline version of FAST does not include TEFs as an input to the rotor; therefore a modified version developed by Sandia National Laboratories is used to simulate the smart rotor control approach. The control design is implemented for the NREL 5MW wind turbine, a widely used research model. The scope of this research is intended to address the following questions:

- How does implementing individual pitch control (IPC), individual flap control (IFC) and a HYBRID controller (combined IPC and IFC), in above and below rated conditions affect the mitigation of blade loads? The efficiency of the controllers are analyzed for both low and high turbulent wind cases along with the load reduction potential, and compared to standard control cases with either no control or collective pitch control.
- How does the presence of smart rotor control affect the aerodynamics of the turbine, and therefore the rotor dynamics? The actuators for blade pitch and TEF cause changes in the coefficients of lift, drag and power for the rotor. Can a strategy be developed to track the changes in the rotor aerodynamics from the smart rotor control algorithms to improve power capture?
- Is the relationship between power output and load reduction inversely proportional? Is there a definite tradeoff between the two that can be bridged in order to have

improved performance? Or does one have to be sacrificed in order to maximize the other?

- Is the standard control law for generator torque for Region 2 still optimum with the addition of dynamic complexities presented by smart rotor control algorithms? The generator torque gain K is analyzed in order to obtain conclusive evidence that there is a superior approach to regulate the generator torque.

CHAPTER 2

MODELING AND PROCEDURE

This section describes the modeling and procedure required to simulate the operation of a wind turbine with smart rotor control actuators. These simulations utilize the IPC, IFC or HYBRID controllers for load alleviation, as well as the various generator torque control algorithms that are tested to improve Region 2 power capture. The turbine is simulated in a modified version of FAST that allows TEF angles as an additional plant input. Additional wind turbine codes that act as preprocessors are used to aid the design and analysis of the turbine as well as the controllers.

2.1 Wind Turbine Modeling

2.1.1 NREL 5MW Wind Turbine

The turbine model used for this research is the National Renewable Energy Laboratory (NREL) 5 MW wind turbine, whose specifications are available through NREL and the National Wind Technology Center (NWTC) [4]. For the purpose of this research, the 126 m diameter, variable speed, 3 bladed turbine is analyzed at an onshore site, to focus on the rotor and generator, while neglecting complexities that arise from offshore analysis. Further specifications for the NREL 5 MW are shown in the Table 2.1 below.

Table 2.1: Design characteristics for the NREL 5MW wind turbine [4]

Rating	5 MW
Rotor Orientation, Configuration	Upwind, 3 Blades
Control	Variable Speed, Collective Pitch
Drivetrain	High Speed, Multiple-Stage Gearbox
Rotor, Hub Diameter	126 m, 3 m
Hub Height	90 m
Cut-In, Rated, Cut-Out Wind Speed	3 m/s, 11.4 m/s, 25 m/s
Cut-In, Rated Rotor Speed	6.9 rpm, 12.1 rpm
Rated Tip Speed	80 m/s
Overhang, Shaft Tilt, Precone	5 m, 5°, 2.5°
Rotor Mass	110,000 kg
Nacelle Mass	240,000 kg
Tower Mass	347,460 kg
Coordinate Location of Overall CM	(-0.2 m, 0.0 m, 64.0 m)

2.1.2 Trailing Edge Flaps

A standard version of FAST is available through NREL that has a baseline collective pitch controller, and generator torque controller. However, the version of FAST used for simulation in this research was developed by Sandia National Laboratory and allows for flap deflection as an additional input for the wind turbine plant. Through a previous design by Lackner [6], the TEF's are added to the outer 70% to 90% span of the blades with the ability to deflect ± 10 degrees.

Aerodynamic tables were created by Lackner using XFOIL, a design tool for the analysis of subsonic isolated airfoils [6]. Essentially, these tables contain lift and drag coefficients, C_l and C_d , according to the angle of attack and flap deflection for the airfoil, which in this case is a NACA 64618. These aerodynamic tables are later used to evaluate forces on the rotor in a subroutine for FAST.

2.2 WT_Perf

In order to quantify the effects of the TEF's on the power performance of a turbine, WT_Perf is used to predict the performance of the rotor. WT_Perf uses blade element momentum theory (BEM), a commonly used aerodynamic analysis technique for wind turbines.

To view the dependence of the power coefficients on TEF angle, tip speed ratio is varied while holding blade pitch constant. This is because in Region 2, the blades are fixed at the optimum pitch angle, in order to have the ideal aerodynamic conditions, resulting in the highest lift to drag ratio. WT_Perf does not allow for aerodynamic tables to be inputted as matrices, so individual tests are simulated for each TEF deflection angle from -10 to +10 in order to create the surface shown in Figure 2.1.

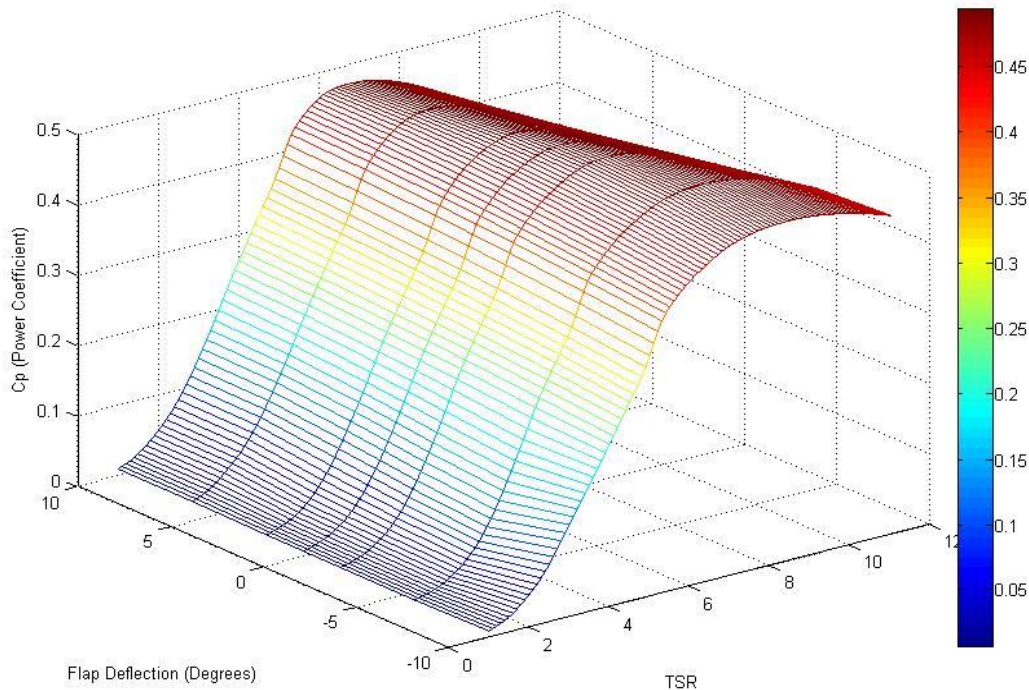


Figure 2.1: C_P vs. λ (Tip Speed Ratio) mesh for varying flap deflection angle

As one can see from the $C_P - \lambda - \theta_F$ mesh, deflecting the flaps in any direction away from 0 degrees results in a lower C_P value. Further analysis of the aerodynamic tables created by XFOIL illustrates a less than optimal lift to drag ratio for any deflection angle away from 0. These C_P values for varying flap angle from the mesh are necessary for generator torque gain analysis, investigated further in this thesis.

2.3 Turbsim

An additional tool required for this analysis is Turbsim, a stochastic, full field, turbulent wind simulator. Turbsim wind files are created with specified mean wind speeds, wind shear exponents, and turbulence intensities. Many wind files are simulated for this research, namely constant wind and full turbulent files for examination of the load reduction capacity of the smart rotor control algorithms. Additionally, the wind speed ranges are specifically chosen so that below rated and above rated operation can be examined separately.

2.4 Aerodyn

The final tool acting as a preprocessor to FAST is Aerodyn, an aerodynamics software module for aero-elastic analysis of wind turbine models. Essentially, Aerodyn acts as an aerodynamic calculator of loads for the blade. It uses a more advanced analysis of blade element momentum theory, compared to that of WT_Perf, resulting in a more accurate representation of turbine performance.

The blade design for this research is identical to that of the NREL 5MW, except with the outer 70-90% of the blade having TEF's and therefore using the data created by XFOIL for the TEFs, which can be seen in Table 2.2 below [6].

Table 2.2: Aerodynamic blade properties for modified NREL 5 MW wind turbine with the addition of TEF [6]

Rnodes (m)	AeroTwst (deg)	Chord (m)	Airfoil
2.866	13.308	3.542	Cylinder1
5.600	13.308	3.854	Cylinder1
8.333	13.308	4.167	Cylinder2
11.750	13.308	4.557	DU40_A17
15.850	11.480	4.652	DU35_A17
19.950	10.162	4.458	DU35_A17
24.050	9.011	4.249	DU30_A17
28.150	7.795	4.007	DU25_A17
32.250	6.544	3.748	DU25_A17
36.350	5.361	3.502	DU21_A17
40.450	4.188	3.256	DU21_A17
44.550	3.125	3.010	TEF
48.650	2.319	2.764	TEF
52.750	1.526	2.518	TEF
56.166	0.863	2.313	TEF
58.900	0.370	2.086	TEF
61.333	0.106	1.142	NACA64_A17

Along with the other aerodynamic properties, such as air density and kinematic viscosity, designated in the Aerodyn input file, the tools necessary for the simulation of this research are now ready for FAST.

2.5 FAST

FAST (Fatigue, Aerodynamics, Structures and Turbulence) is an aeroelastic code capable of simulation and linearization of both two and three bladed horizontal axis wind turbines. The code contains multiple states and degrees of freedom to analyze the non-linearities of wind turbine dynamics. It has the ability to calculate various loads on the rotor-nacelle-hub assembly (RNA), as well as the tower. Additionally, FAST can evaluate both onshore and offshore cases, but for the purpose of this research, offshore tests are not evaluated.

FAST has the ability to be run through Simulink for additional signal processing and controller design. The modified version of FAST that is used in this research allows turbine plant inputs of generator torque, generator power, yaw position, yaw rate, blade pitch angles and TEF angles. A schematic of the model is shown below in Figure 2.2.

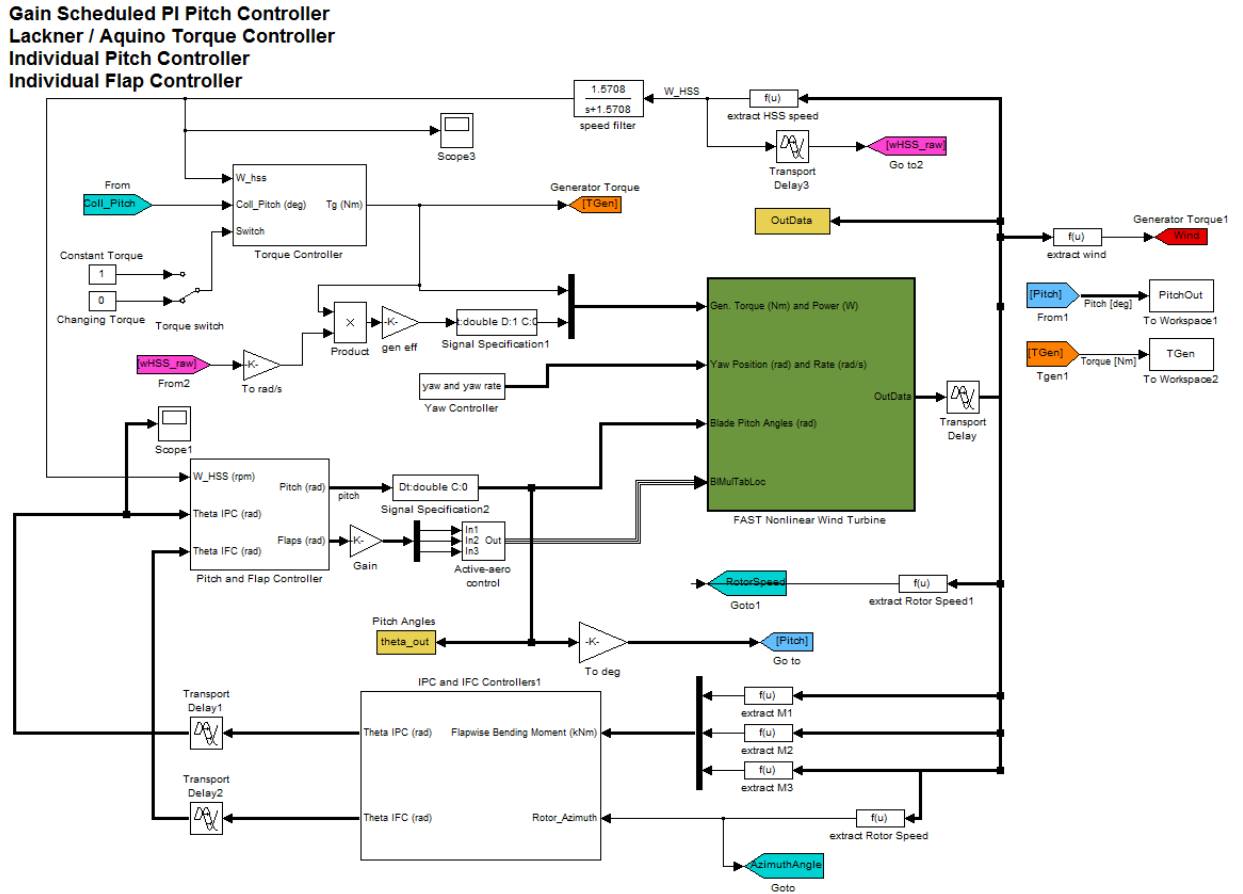


Figure 2.2: Overview of FAST model for simulations

Figure 2.2 shows the closed loop system with multiple inputs and multiple outputs (MIMO), where wind acts as a disturbance to the system. The green block is the wind turbine plant that contains the dynamics of the turbine and its components. Additionally, two controllers are standard with the Simulink model, a collective pitch controller and a torque controller. For this research, collective pitch is not examined because of the focus on smart rotor control strategies such as IPC and IFC.

The generator torque controller for this model uses a generic strategy. When the shaft reaches the cut in rotational speed, where the generator can then begin to produce power, the torque

is matched proportionally to the optimal tip speed ratio and C_P by the gain K , which has been discussed previously. For this turbine model, it is suggested to use a gain of $K= 0.02556 \text{ N}\cdot\text{m}/\text{rpm}^2$ to calculate torque using Equation 1.2. In Region 3, the torque is inversely proportional to the rotor speed of the turbine, therefore keeping power constant through operations in higher wind speeds.

CHAPTER 3

ADVANCED CONTROL DESIGN

This chapter explains the modeling and procedural process of the advanced controllers applied to the NREL 5MW wind turbine. The smart rotor controllers for fatigue reduction include Individual Pitch Control (IPC), Individual Flap Control (IPC) and coupled IPC plus IFC Controller (HYBRID). In addition, various generator torque control methods are also described, with the aim to overcome the power loss that occurs from the smart rotor controllers.

3.1 IPC and IFC Control Strategy

More advanced control algorithms than collective pitch control, which is referred to as standard control (SC), are necessary to enhance the load reduction capabilities of turbine controls. This section explores the methodology of both IPC and IFC, which are in fact identical in nature.

A feedback control approach is taken for the control design of the IPC and IFC controllers designed by Lackner [6], with the controller output angles a function of individual blade root bending moments (M_{y1} , M_{y2} , M_{y3}). The difficulty with this approach is that the blades are in a rotating reference frame, containing periodic terms that make the system linear time varying (LTV). In order to simplify the control design process, which in this case is a PID control, the system must be converted to a linear time invariant model, with a fixed reference frame [2] [6].

An approach widely implemented in helicopter applications, as well as wind turbine control design, is the Coleman Transform. This is a multi-blade transformation that converts a rotating coordinate system into a fixed nacelle-tower coordinate system with no periodic terms. Although

there is some ambiguity behind the effectiveness of this method, it is commonly accepted that this transformation is suitable for PID control designs, which are implemented in this research [2] [6]. The Coleman matrix P , and its inverse P^{-1} , are shown in the Equations 3.1 and 3.2. The rotor azimuth angle, ψ , describes the position of each blade where 0° , 120° and 240° are the positions when one blade is pointed directly upwards.

$$P = \begin{pmatrix} 1 & \sin\psi_1(t)\cos\psi_1(t) \\ 1 & \sin\psi_2(t)\cos\psi_2(t) \\ 1 & \sin\psi_3(t)\cos\psi_3(t) \end{pmatrix} \quad (3.1)$$

$$P^{-1} = \frac{1}{3} \begin{pmatrix} 1 & 1 & 1 \\ 2\sin\psi_1(t) & 2\sin\psi_2(t) & 2\sin\psi_3(t) \\ 2\cos\psi_1(t) & 2\cos\psi_2(t) & 2\cos\psi_3(t) \end{pmatrix} \quad (3.2)$$

When a vector variable is multiplied by the inverse Coleman P^{-1} from Equation 3.4, it is transformed into the fixed frame coordinate system, and when multiplied by P in Equation 3.3, it is returned to its rotating frame. For these two controllers, M_{y1} , M_{y2} and M_{y3} are the variables that must be transformed into the fixed reference frame in order for the individual pitch angles, θ_{P1} , θ_{P2} , θ_{P3} , and individual flap angles, θ_{F1} , θ_{F2} , θ_{F3} , to be controllable based on that signal. When variables of each blade are transformed into the fixed reference frame, they are designated with the superscript CM. The subscripts 2 and 3 for the bending moments in the fixed frame represent the yaw wise and tilt wise moment of the rotor. The tilt wise moment is most important because wind shear loading on blades tends to dominate the fatigue and produces primarily a tilting moment. For this control strategy, the average moment, M_{yI}^{CM} , is ignored.

$$\begin{bmatrix} \theta_1(t) \\ \theta_2(t) \\ \theta_3(t) \end{bmatrix} = \begin{bmatrix} 1 & \sin\psi_1(t)\cos\psi_1(t) \\ 1 & \sin\psi_2(t)\cos\psi_2(t) \\ 1 & \sin\psi_3(t)\cos\psi_3(t) \end{bmatrix} \begin{bmatrix} \theta_1^{cm}(t) \\ \theta_2^{cm}(t) \\ \theta_3^{cm}(t) \end{bmatrix} \quad (3.3)$$

$$\begin{bmatrix} M_{y1}^{cm}(t) \\ M_{y2}^{cm}(t) \\ M_{y3}^{cm}(t) \end{bmatrix} = \frac{1}{3} \begin{bmatrix} 1 & 1 & 1 \\ 2\sin\psi_1(t) & 2\sin\psi_2(t) & 2\sin\psi_3(t) \\ 2\cos\psi_1(t) & 2\cos\psi_2(t) & 2\cos\psi_3(t) \end{bmatrix} \begin{bmatrix} M_{y1}(t) \\ M_{y2}(t) \\ M_{y3}(t) \end{bmatrix} \quad (3.4)$$

With the root bending moments, M_y , now transformed into a Coleman variable in the fixed frame, a control approach created by Lackner [6] can now be implemented for the pitch and flap angle calculations. A PID controller is implemented in this controller design, due to its simplicity and proven efficiency by several authors such as Lackner and Andersen [1, 6]. The PID control algorithm has three different gains: proportional gain for the immediate response of the signal, integral gain for the response over the entire signal series, and derivative gain for predicting oncoming signals. The controller function for input M^{CM} and the output θ^{CM} are shown in Equation 3.5.

$$\theta^{CM} = K_p M^{CM} + K_D \dot{M}^{CM} + K_I \int_0^t M^{CM} dt \quad (3.5)$$

However, due to the wide range of the root bending moment due to winds varying from 3 m/s to upwards of 20 m/s, precautions must be taken to ensure that the pitch and flap angles do not saturate to their maximum values. Doing so would result in a constant non-ideal operating condition that will compromise rotor performance. A widely used technique to avoid saturation is gain scheduling, where the gains are proportioned based on the value of a separate input variable

[6]. In this case, wind speed is used to find the optimal gain scheduling values for improved controller performance. Through multiple test simulations under various wind speeds, the initial gains and proportional gain scheduled values are calculated and are shown in Tables 3.1 and 3.2 below for both the IFC and IPC controllers.

Table 3.1: PID controller gains for IPC and IFC

	IPC	IFC
Proportional gain	1.00E-08	-1.00E-03
Integral gain	1.50E-09	-5.00E-04
Derivative gain	1.00E-08	-3.00E-04

Table 3.2: Gain scheduled values for IPC and IFC controllers

	< 7 m/s	7 - 9 m/s	9 - 12 m/s	12 -14 m/s	> 14 m/s
Gain Schedule	1.00	0.85	0.65	0.55	0.40

Intuitively, gain scheduling affects the sensitivity of the controller because at higher wind speeds a given change in the flap angle results in a larger change in lift. The feedback control structure for the IPC and IFC is shown in the schematic below in Figure 3.1.

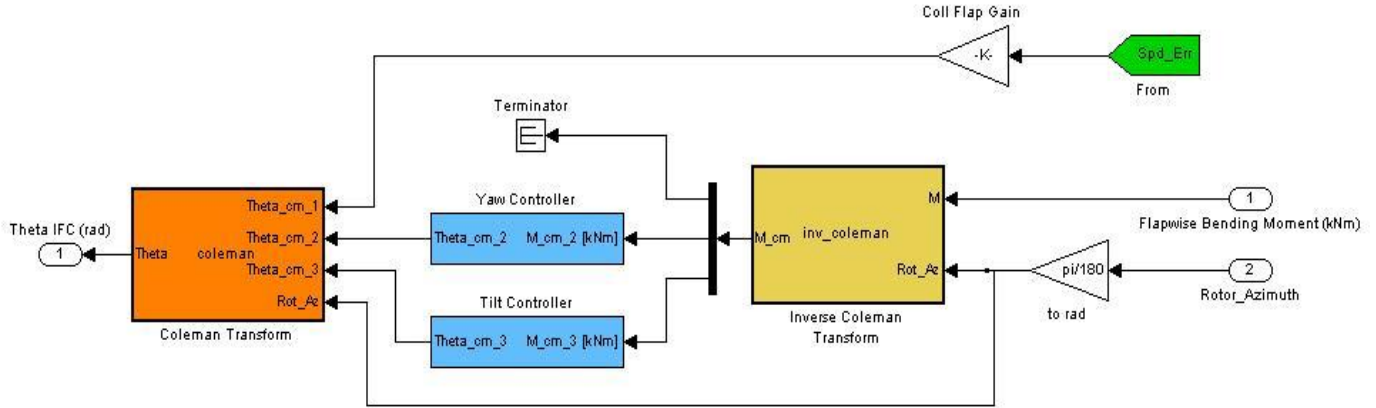


Figure 3.1: Schematic of control design for IPC and IFC controllers

The control algorithm procedure in detail is:

- The root bending moment M_y and rotor azimuth angle ψ are fed into the inverse Coleman matrix P^{-1} , represented as the yellow embedded function. The azimuth angle is used to map the position of the individual blades. M_y in the rotating reference frame is transformed into its Coleman representation where it is now mapped into a fixed frame of tilt and yaw coordinates.
- The M^{CM}_2 and M^{CM}_3 are utilized in their respective controllers, represented in light blue, where the PID algorithm with gain scheduling is applied. The controller outputs the variables θ^{CM}_2 and θ^{CM}_3 .
- θ^{CM}_2 and θ^{CM}_3 are processed in the Coleman matrix P , and transformed back into the rotating reference frame, which are then used to calculate separate flap and pitch deflection angles for each blade. This signal is then input to the wind turbine plant.

3.2 Proposed Generator Torque Control for Region 2

3.2.1 Gain Reduction of Generator Torque

As previously noted, work done by Johnson et al. suggests using a reduced generator torque gain to match the gusts and lulls of turbulent wind for improved performance [5]. The rotor spends much of its time attempting to regulate its rotation in order to operate at its optimal point, which is $\lambda = 7.55$ for the NREL 5MW.

To test this method, the generator torque is decreased between 1-20% for below rated wind speeds with varying turbulence intensities. While this approach has proven successful in SC environments for Region 2, this has yet to be simulated with smart rotor controllers. Standard Region 2 control operation actually has no rotor control devices activated (collective pitch and IPC are Region 3 controllers), so for this simulation the IFC is the only controller implemented. The results of both cases, SC and IFC, are compared.

3.2.2 Wind Speed Standard Deviation Torque Controller

After testing the potential of generator torque gain reduction, a more intuitive approach towards generator torque control is examined. As stated in the previous section reducing the generator torque helps the rotor to adjust to the gust and lulls of the wind to better match its optimal tip speed ratio [5]. However, by constantly holding the generator torque lower than its designed value, the generator is not operating at its optimal point during much of its operation. Consequently, outside of the instances where there are high variations in the wind, the generator produces less power due to the decrease in generator torque during steadier wind periods.

A more intuitive approach to control the generator torque to adjust to the wind turbulence is proposed by Balas et al. [2]. It suggests a control strategy based on the standard deviation of the wind speed. Although wind speed is a disturbance that cannot be accurately measured at present time steps, the variance of previous time windows of wind speed can be calculated to predict the oncoming turbulence intensity of the wind. During highly turbulent periods this knowledge may be used to decrease the generator torque, and increase it when the wind speeds reach steadier states.

The advantages of this control method can be realized by conceptualizing how the rotor reacts to highly turbulent winds. When a large gust of wind passes the turbine, the wind speed rapidly increases while the rotor attempts to adjust its speed to operate at its optimal tip speed ratio. During that time period of sudden wind speed increase, the tip speed ratio of the rotor decreases, which can be seen by Equation 1.1. However, once the gust passes, the rotor is able to accelerate or decelerate towards its optimal tip speed ratio.

Though these time periods are short, the optimal generator torque gain K is highly reliant on the tip speed ratio of the rotor. Power loss occurs at these time windows due to sub optimal tip speed ratio operation. Referring to Equation 1.5, the gain K is heavily reliant on tip speed ratio because it is a function of λ^3 , so operating closer to the optimal value of K even for short periods of time can result in improved power production.

A generator torque controller is designed based on the past wind speeds that are measured by the turbine in FAST. The controller is a function of different variables to accurately measure the wind variance. Along with having wind speed as an input, the sampling frequency of the controller can also be tuned. All the simulations for this research have a maximum sampling frequency of 80 Hz, or one data point per every 0.0125 seconds. The variance between each one

of these time steps may be negligible, so the time steps for the standard deviation of the wind can be modified by the user. For the initial testing of this controller, the frequency of the wind samples is decreased to 1 Hz because the variation of wind speed for larger sampling frequencies are minimal and negligible.

In addition to this, the sample size of the standard deviation period can also be modified. By varying the sample size, an optimal time period can be found that gives the most accurate time series representation of wind turbulence that may affect the rotor performance. With these designated control inputs, the function of the controller can be seen in Equation 3.6.

$$STD_K = STDevaluation (binSize, f, u) \quad (3.6)$$

The controller is designed in Simulink and the outputs are fed into the standard generator torque controller of the NREL 5MW to adjust the torque gain. A rate limiter is utilized to damp out the high rates of change in generator torque that the rotor cannot respond to. A schematic of the controller can be seen below in Figure 3.2.

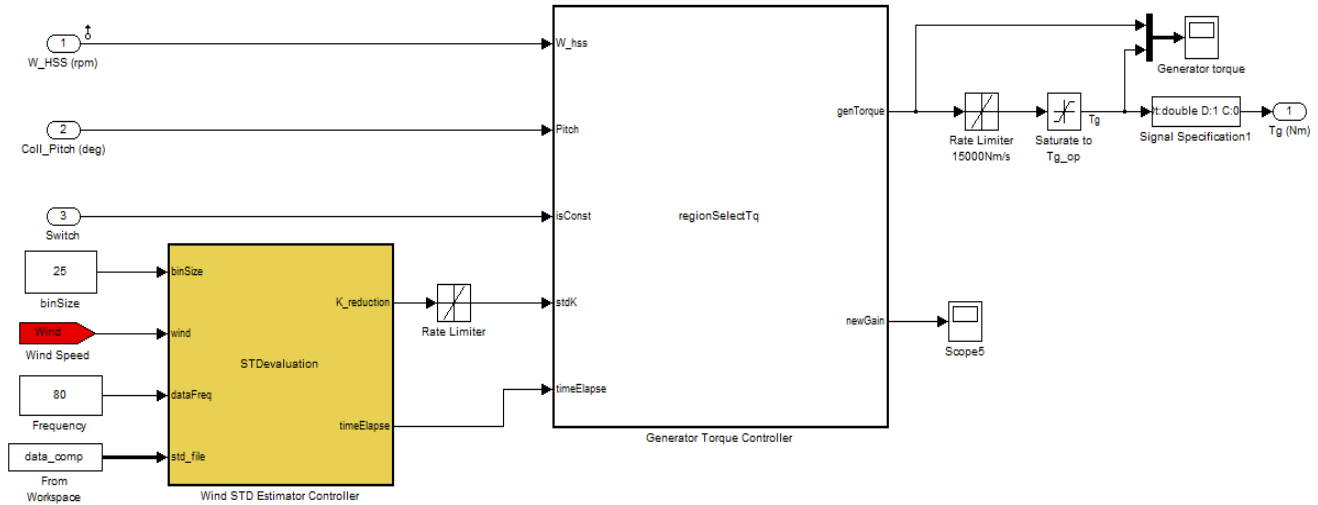


Figure 3.2: Schematic of Wind Standard Deviation Torque Controller

3.2.3 Tip Speed Ratio Tracking Control

The next methodology implemented is a tracking controller that also attempts to control generator torque to improve power performance. A scheme proposed by Johnson [5] states that there is a power loss deficit of about 1% to 3% due to the turbine not operating at its optimal tip speed ratio. As previously reviewed, this issue is due mostly to the rotor adjusting to the variances in wind speeds. The delayed response of the rotor to the instantaneous change in wind speed causes the turbine to deviate from its optimal operating point. This tracking control method uses error estimation based on the optimal design operating points of the system to more accurately calculate generator torque for the turbine.

By manipulating generator torque, the rotor improves its power capture by operating closer to its optimal operating point. By tracking the error of the actual tip speed ratio from its optimal point, the gain K may vary and send inertia into the shaft to either accelerate or decelerate the rotor

closer optimal tip speed ratio [9]. For example, if the tip speed ratio is above its set point, the generator torque can be increased to slow down the rotor and decrease tip speed ratio, so that it is closer to that value. The rotor thus has a faster response due to the torque control gain command, as opposed to the slower response from holding the gain constant.

The proposed controller design is a real time error estimation function based on the current tip speed ratio and a tip speed ratio set point that can be edited by the user. For the purpose of this research, a set point tip speed ratio of 7.55 is used, as it is the optimal tip speed ratio for the NREL 5 MW wind turbine [4]. The gain adjustment is inputted into the standard generator torque controller provided by FAST which can be seen in Figure 3.3.

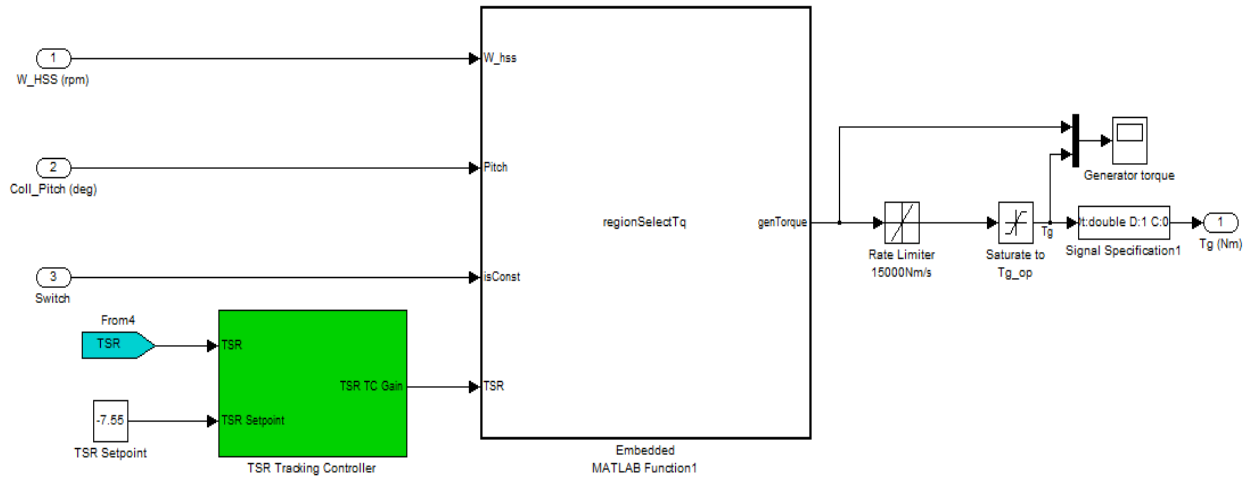


Figure 3.3: Schematic of Tip Speed Ratio Tracking Controller

3.2.4 Power Production Sensitivity with Wind Speed Estimation Error

The previous sections have all highlighted control techniques that focus on having wind speed as an instantaneous and accurate measurement. While FAST allows wind speed to be

measured at the current time step, this is not always the case in real life situations. Although wind turbines are equipped with wind measurement devices, the accuracy of these devices is less than what is available in the FAST simulations.

In order to test the efficiency of the Tip Speed Ratio Tracking Controller, a sensitivity analysis to wind speed estimation error is utilized. As previously noted, measuring wind speed can be difficult and inaccurate, which makes it less logical to use as a control input to a control algorithm. Therefore, in this method a degree of wind speed error is added to the controller in order to observe the sensitivity of the control approach to wind speed estimation error.

The function to introduce the error in the Tip Speed Ratio Tracking Controller is based on Equation 1.1. The controller is tested by adding a specified amount of error to the wind input, which is used to recalculate the tip speed ratio with the error introduced to Equation 3.7.

$$\lambda_{error} = \frac{\omega R}{u (1 \pm error \%)} \quad (3.7)$$

The value λ_{error} is used as an input to the TSR Tracking Controller to simulate the error in attempting to measure and predict wind speeds, which can be seen in Figure 3.4.

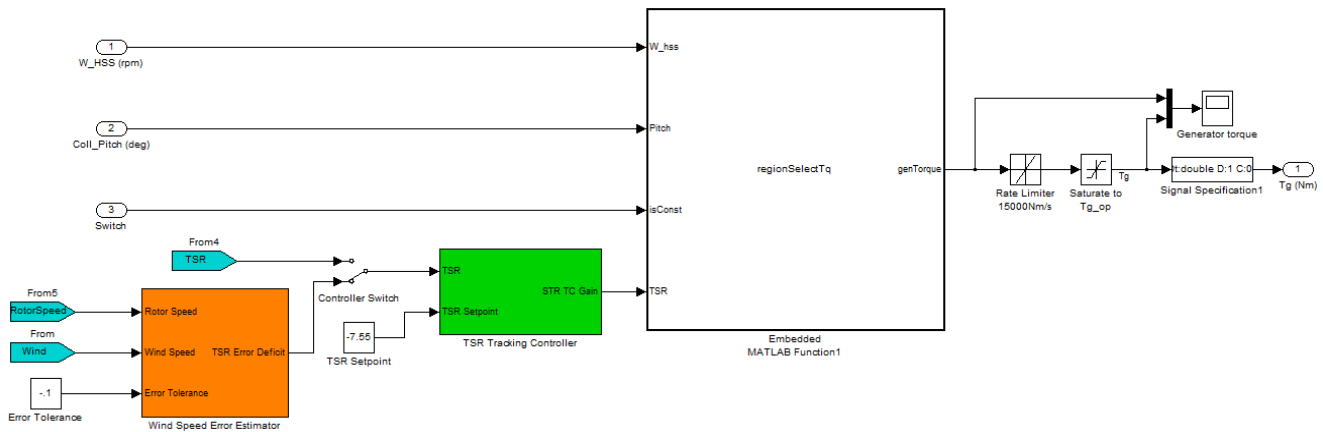


Figure 3.4: Wind Speed Error Estimation Controller

The controller assumes that the tip speed ratio input is the correct measurement of the turbine, therefore introducing λ_{error} causes the magnitudes of the gains to differ.

The simulations are conducted with a range of 1% to 20% wind speed error to test the robustness of the controller. These results are compared to the baseline case where the true tip speed ratio is used as an input.

3.2.5 Smart Rotor Torque Regulator

The proposed control technique in this section is an error estimation function coupled with knowledge of how the smart rotor control algorithms in Region 2 affect the rotor speed. The set point of this controller is based on the operating points of Region 2, most importantly a tip speed ratio of $\lambda = 7.55$.

The influence of smart rotor control on the dynamics of the turbine can be quantified by analyzing the Coleman angles that are used in the PID controller for IFC. θ^{CM}_3 impacts the tilting moment, and has the most influence on the IFC command in most cases due to wind shear. Figure 3.5 is created by using steady wind to illustrate the periodic response of the IFC controller, strictly due to wind shear. The θ^{CM}_3 is a 3P signal, with peaks that represent the position of a blade at 0 degrees, shown at time step 96, where the blade has the greatest root bending moment due to wind shear. Consequently, at this point, the controller outputs the largest TEF deflection angle.

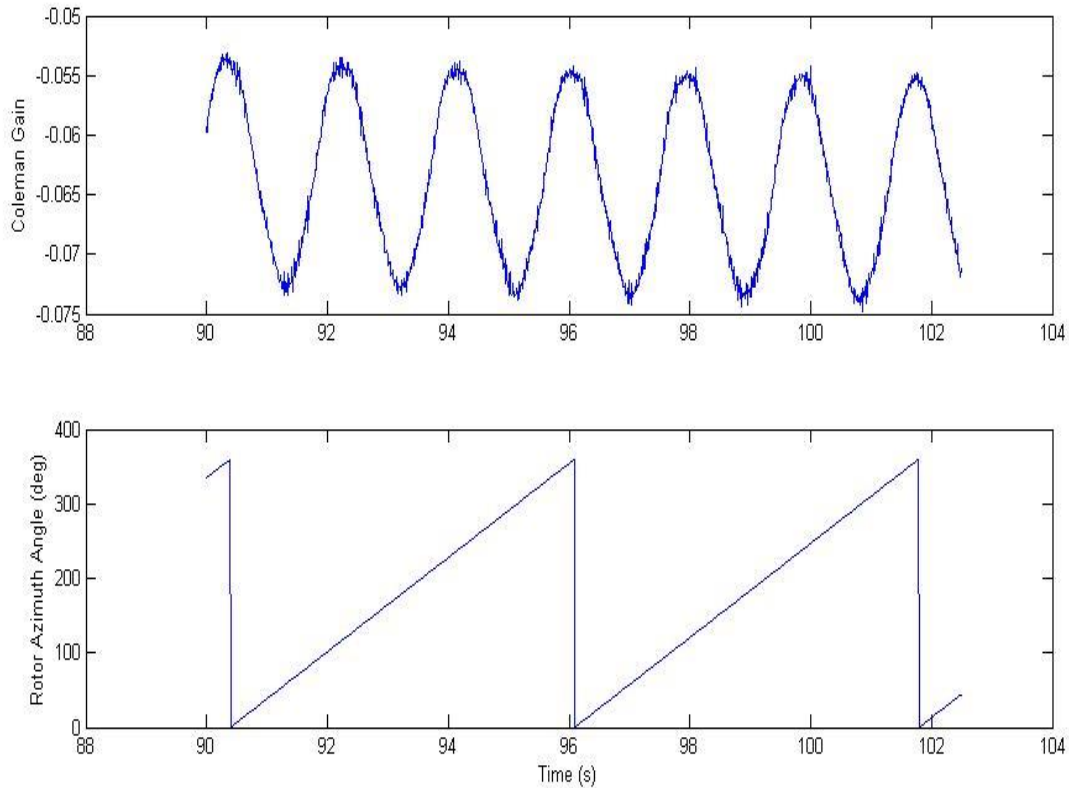


Figure 3.5: Coleman tilt angle and rotor azimuth angle for steady wind case

Due to the maximum tilt moment causing the TEF to deflect to its maximum angle at this point, the overall aerodynamic performance of the rotor is reduced as the lift to drag ratio is minimized. This reduction in lift to drag ratio decreases the aerodynamic torque, and causes the speed of the rotor to be the slowest as each blade approaches zero degrees. Using this knowledge, K is adjusted according to the Coleman angle, with the gain increased from position of 0 to 60° where the rotor speed is slowly increasing, and decreased between 60 and 120° where the next blade approaches the 0 azimuth angle. A baseline proportional controller is employed initially for

testing, to avoid integral windup and possible overshoot from the derivative gain. The transfer function for this controller is shown below in Equation 3.8.

$$K_{SRTR} = K_P \lambda + K_{CM}(\theta_3^{CM}) \quad (3.8)$$

This newly calculated K is inputted into the generator torque controller for Region 2 operation. A schematic of the controller layout is shown below in Figure 3.6.

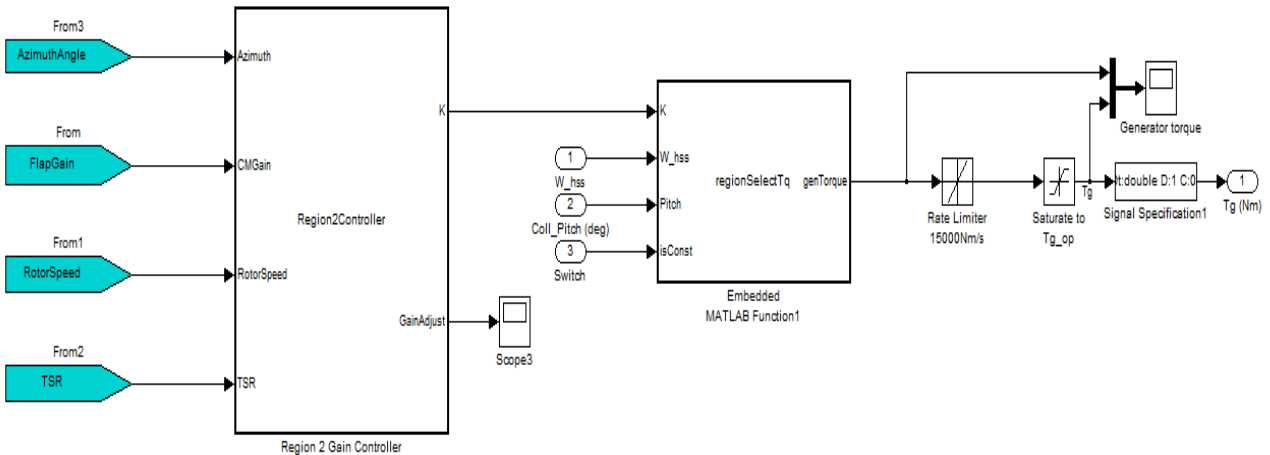


Figure 3.6: Schematic of Smart Rotor Torque Regulator (SRTR) controller

3.2.6 Recalculating K Based on C_P for Varying Flap Deflection Angles

Power coefficient calculation is the focus of this sections methodology. C_p for a rotor varies for different blade properties, such as blade pitch and tip speed ratio. Figure 3.7 depicts how the power coefficient can vary based on both of these properties.

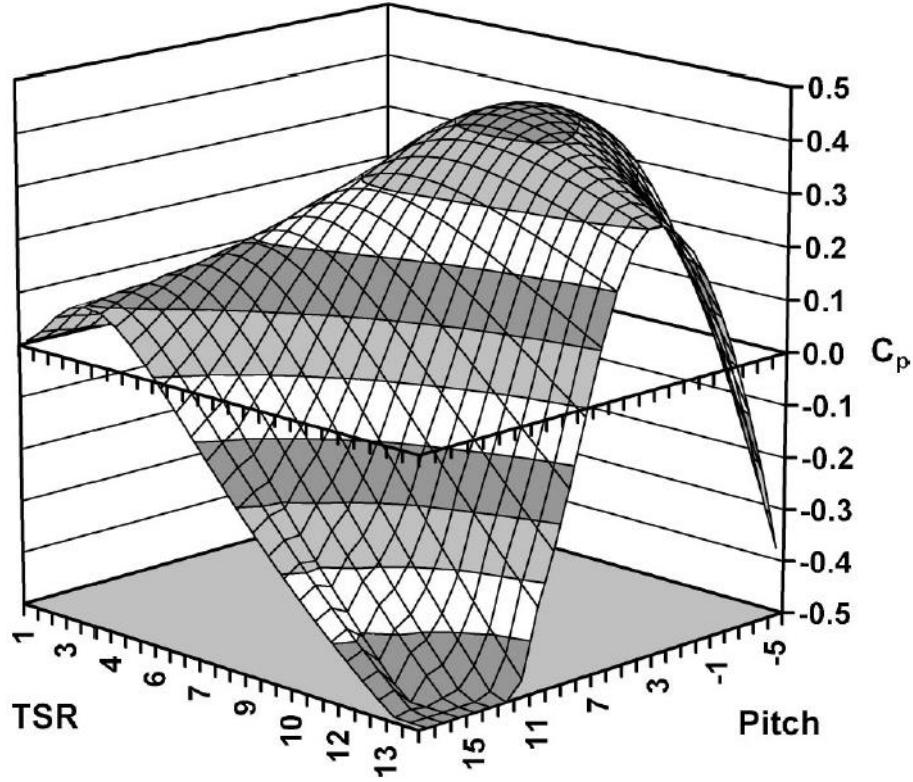


Figure 3.7: C_P vs Pitch Angle vs TSR mesh. An example of how power coefficient can vary with pitch angle [9]

A mesh such as this one can be calculated using WT_Perf, assuming that the properties of each blade are uniform. The calculation of the C_P values are important because it is used to calculate the optimal gain in Region 2, as seen in Equation 1.5.

With the addition of the TEFs, the rotor may not be accurately represented by the maximum C_P value that is used in the calculation of K . The value of the gain $K = 0.02556 \text{ N}\cdot\text{m}/\text{rpm}^2$ assumes that the optimal operating point of the NREL 5MW has a $C_P = 0.482$, at a $\lambda = 7.55$ and pitch angle of 0 for each blade. However, this approach does not take into consideration the three different flap deflections of each blade when calculating C_P . As C_P varies with λ and pitch angle in Figure

3.7, it also varies with flap deflection angle as seen in Figure 2.1. No single point on the mesh can be an exact representation of the C_P for the rotor because it is calculated assuming that all the blades have the same flap deflection angle. The schematic in Figure 3.8 illustrates the implementation of the control algorithm. The proposed control algorithm in this section has the following characteristics:

- The inputs to the controller are the three TEF angles of each blade.
- For each TEF angle, C_P is located on the $C_P - \lambda - \theta_F$ mesh and the three values are averaged to create a collective C_P value. This assumes that the C_P of the rotor with three different TEF angles on each blade is similar to the average of three different C_P 's from three separate rotors that have uniform TEF angles corresponding to the three controller inputs. For example, if the three input TEF angles are -10, 0 and 10 degrees, the controller averages the C_P from three different rotors with collective TEF angles of -10, 0 and 10 degrees respectively.
- K is recalculated at every time step with this collective C_P value.

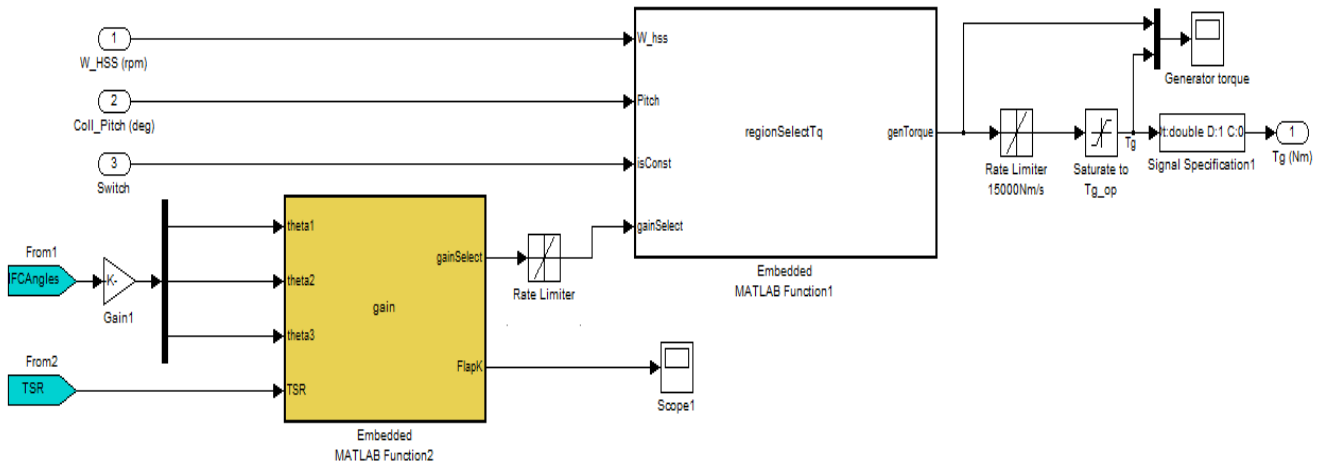


Figure 3.8: Schematic for Optimal TEF CP Controller

Due to the high frequency of the simulation, a rate limiter is used to reduce the noise that occurs from calculating the gain each time step. There is no variation in C_P due to blade pitch angle, because it is held constant at 0 in Region 2. Figure 3.9 is an example of how averaging the different C_P values for each blade affects the overall power coefficient of the rotor for this approach. The C_P versus λ curves in this figure are taken from the mesh created by WT_Perf in Figure 2.1. The dotted line represents the average power coefficient of the rotor based on the three separate power curves from the corresponding flap deflection angles of each blade.

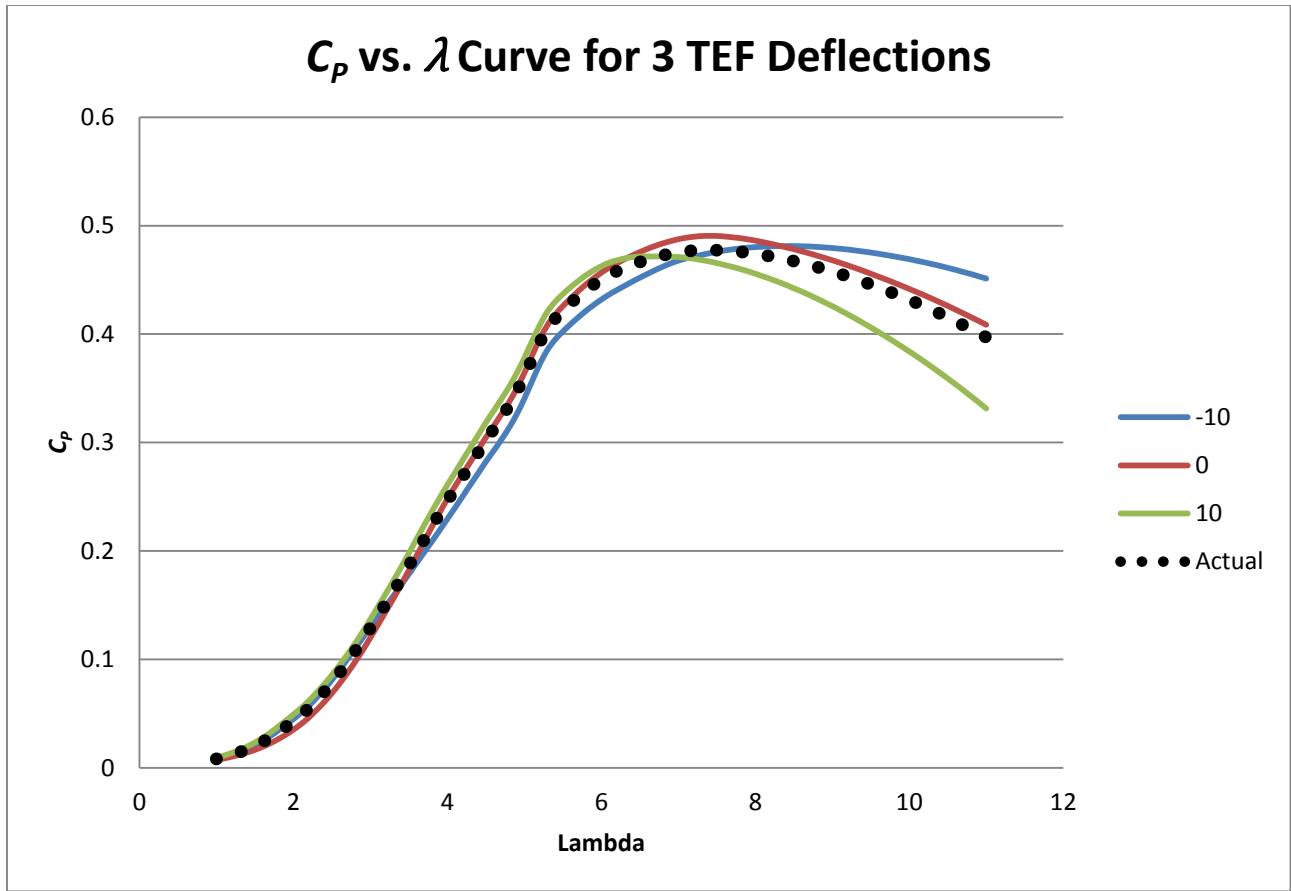


Figure 3.9: Example of real time calculated K value for blades deflecting at different flap angles

3.2.7 Linear Quadratic Regulation Control

An alternative and more complex approach to control design is linear quadratic regulation control (LQR), a type of state space feedback controller. The theory behind LQR control is that the cost function of some process can be regulated by assigning weighted importance to the outputs. The algorithm finds gain values that minimize deviations from the output. Matlab has a built in LQR control design function that requires a linearized state space model of a system and the weighted cost matrix for optimization.

An approximate linear state space model for the turbine is created with θ^{CM} and τ as inputs, and M_Y and power as outputs. The state space model representation is shown in the equations below, where x is the state vector, y is the output vector, u is the control vector, A is the state matrix, B is the input matrix, C is the output matrix, and D is the feed through matrix.

$$\dot{x}(t) = Ax(t) + Bu(t) \quad (3.9)$$

$$y(t) = Cx(t) + Du(t) \quad (3.10)$$

Although FAST has an analysis mode for model linearization, the modified version with TEF does not allow this analysis mode to run through Simulink. In order to create a state space model, time series data is created in FAST with steady a 8.5 m/s wind to ensure operation only within Region 2 of the power curve. The data is first formatted into an input-output object based on the time series step size, using the function IDDATA. The state space model is then created using SSDATA in order to extract the A , B , C and D matrices for control design, and is shown in Table 3.3.

Table 3.3: State space matrices for approximate linearization of the turbine model with IFC activated

A		B	
1.004	4.333E-06	-0.017	-1.248E-05
-0.012	0.995	-0.139	3.322E-04
C		D	
1203.751	-64.218	0.000	0.000
32.675	-0.041	0.000	0.000

The weighting of the output matrices can be varied based on regulation of the desired outputs. For this section, the main objective is to improve power capture. An assumption for this

approach is that there is minimal interaction with the two outputs, or the controller would be competing with itself to maximize both outputs unintentionally. A bode plot displays the frequency response of the system in Figure 3.10.

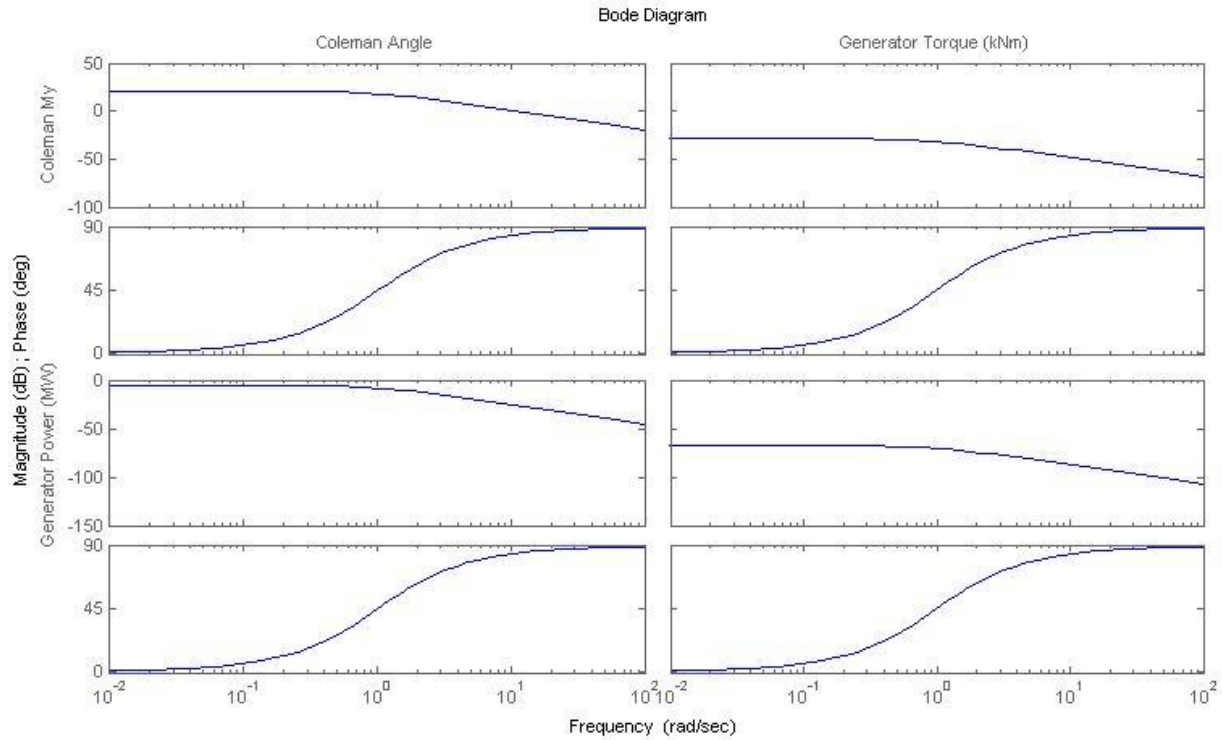


Figure 3.10: Bode plot for frequency response of the linearized turbine model with inputs as Coleman angle and generator torque, and outputs generator power and flapwise root bending moment

As expected, there is a strong coupling between the flap bending moment and generator power, as all of these relationships have the same phase change through identical frequencies. This may lead to the notion that the tradeoff between load reduction and power output is unavoidable. A method to overcome this issue is static decoupling, but for this research may be outside the

scope. With this knowledge of the system, the weighting matrices are varied in an attempt to improve power performance.

In order to verify that this system is controllable, Matlab is utilized to test this through its built in functions. The controllability matrix is found by using the function *ctbr()*, with the argument being the state space model created through Matlab. The controllability of the matrix is found to be 2x2. Therefore, in order for the system to be controllable, the number of states of the system must equal the rank of the controllability matrix. Taking the rank of the matrix results in a value of 2, which matches the states of the system, My^{CM}_3 and *Power*. Thus, the system is controllable and an LQR controller is realizable.

The gains of the LQR controller are based on the weighting of the importance of the outputs of the system. The design of the LQR controller is reliant on the ratio of the Q and R matrices, where the Q matrix represents the state weighting matrix and R represents the control weighting matrix. For this analysis, the simplest solution is to leave R as an identity matrix, while varying the importance of the state matrix values in Q for both My^{CM}_3 and *Power*.

CHAPTER 4

RESULTS AND DISCUSSION

This chapter reviews the results of the time series simulations run using FAST with the controller strategies described in Chapter 3. The first section examines the load reduction capabilities of the IPC and IFC controllers, as well as their effects on power generation and rotor dynamics. Next, the proposed generator torque controllers are tested to examine if the algorithms do indeed have the potential to improve Region 2 power capture, in particular when the IFC controller is also operating.

Each simulation is run for 600 seconds, with the time windows chosen for each figure that best displays the effects of the controller. The first 30 seconds of each FAST simulation are ignored, as it is the time required for initial transients to become negligible.

4.1 Smart Rotor Control Load Reduction Results

Two separate wind files are created using Turbsim for the load alleviation testing of the IPC and IFC controllers. Both files are created with a wind shear power law exponent of 0.14 and a turbulence intensity of 15%. The first file has a mean wind speed of 8.5 m/s, while the second is 13.5 m/s to ensure that the turbines operate solely in Region 2 and 3 respectively, without Region switching. The wind speed time series can be seen in Figure 4.1 below.

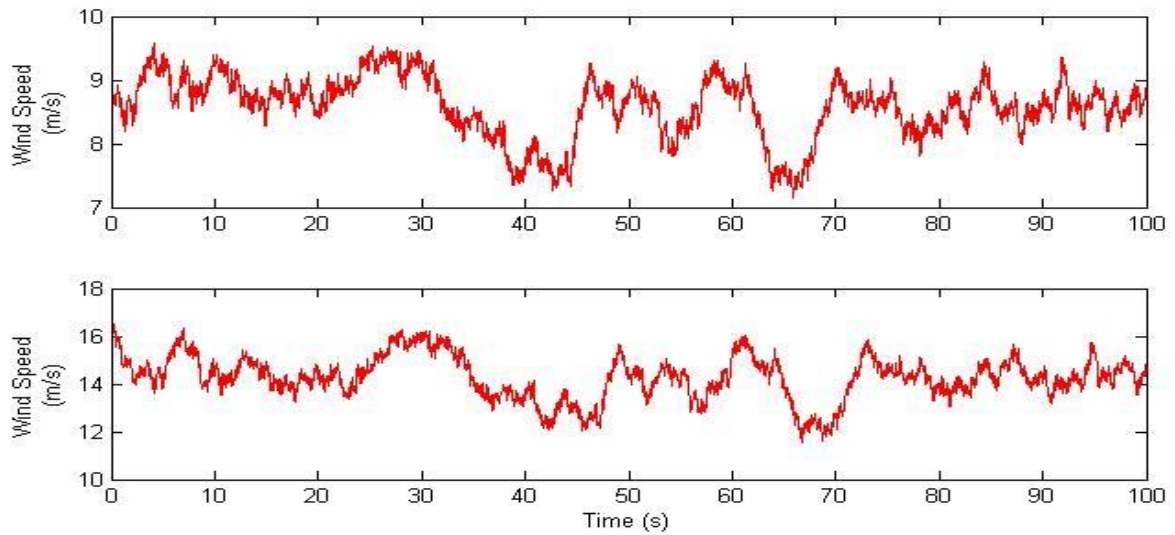


Figure 4.1: Medium turbulent wind data to be used for simulations. Top graph has a mean wind speed of 8.5 m/s, while the bottom has a mean wind speed of 13.5 m/s

4.1.1 Below Rated Results

Region 2 allows for two different control settings for load alleviation, standard control and IFC. The turbine model is simulated using the 8.5 m/s wind file for both cases. The IFC controller is successful in reducing the standard deviation of the blade root flapwise bending moment M_y of the blades by about 12.1%.

As one can see from Figure 4.2, the extreme values, maximum and minimum, of M_y have been reduced because of the IFC controller. Hence, TEFs prove to be an effective approach at mitigating loads

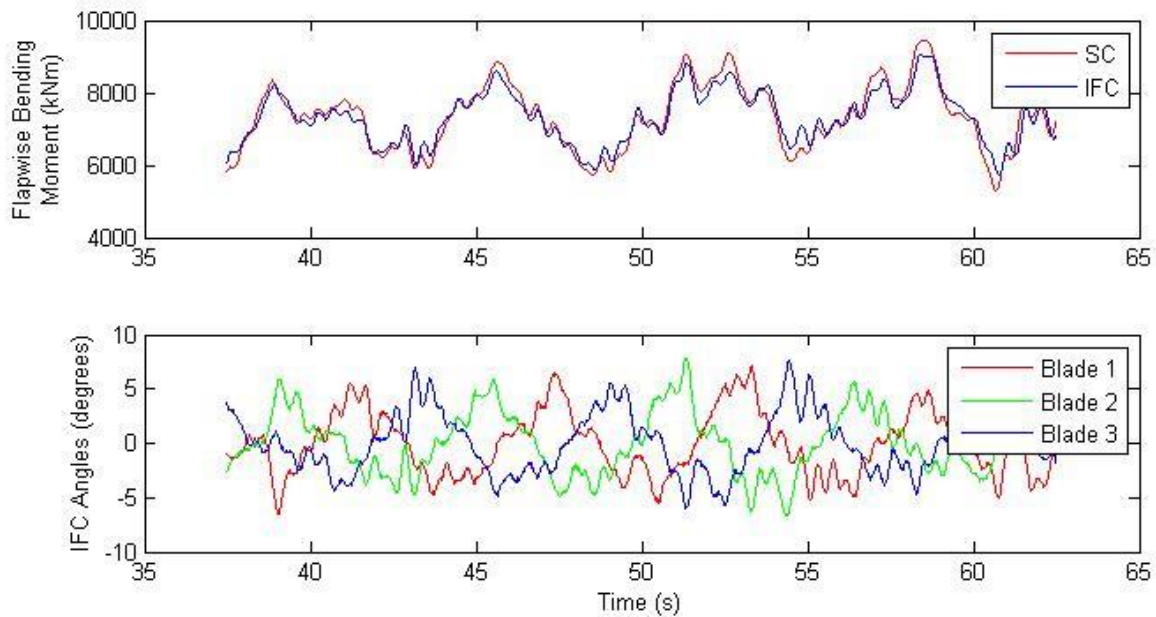


Figure 4.2: Comparison of IFC and SC flapwise root bending moments for blade 1 and IFC commands for each blade in below rated conditions

4.1.2 Above Rated Results

The 13.5 m/s turbulent wind file is used to test the effectiveness of the IPC, IFC, and HYBRID (IFC plus IPC) controllers in Region 3 compared to standard control. In this region, collective pitch commands are used for rotor speed control.

As expected, the HYBRID IPC plus IFC controller is the most successful in reducing the extreme aerodynamic loads on the turbine blades, with a reduction in the standard deviation of the blade root bending moment of 26.3%. IPC reduces the loads by 19.1% and IFC by 13.6%. The time series simulation results shown in Figure 4.3 below demonstrates the load alleviation capability of the IPC, IFC, and HYBRID controllers compared to the standard collective pitch controller.

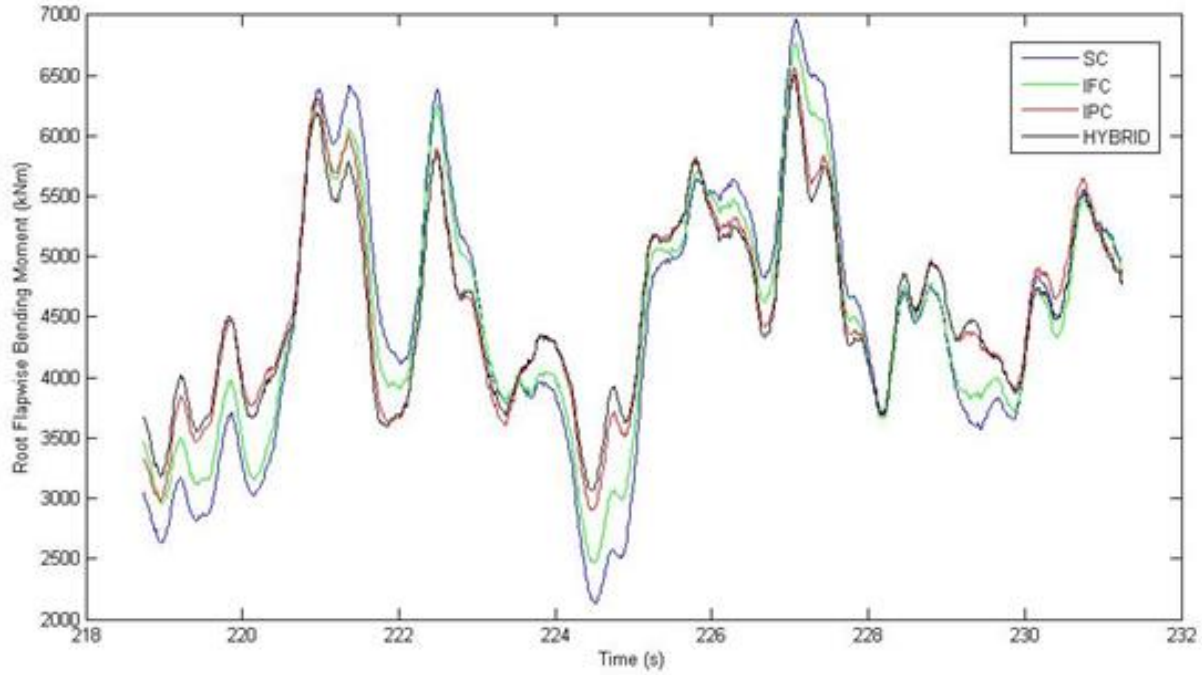


Figure 4.3: Comparison of root flapwise bending moment for SC, IPC and HYBRID controllers for above rated wind speeds

From analyzing the signal of both the IPC and IFC outputs in Figure 4.4, each blade shows a strong 1P signal. Comparing the blade 1 M_y to its flap deflection angle, the signals are 180° out of phase to each other, because of the negative gain assigned to the IFC controller, while the IPC signal is in phase with M_y . The valleys in the IFC signals and the peaks of the IPC signals, one of which occurs at 224.5 seconds, correspond to the blade located at a rotor azimuth angle of 0 degrees, where the load on the blade is largest due to wind shear.

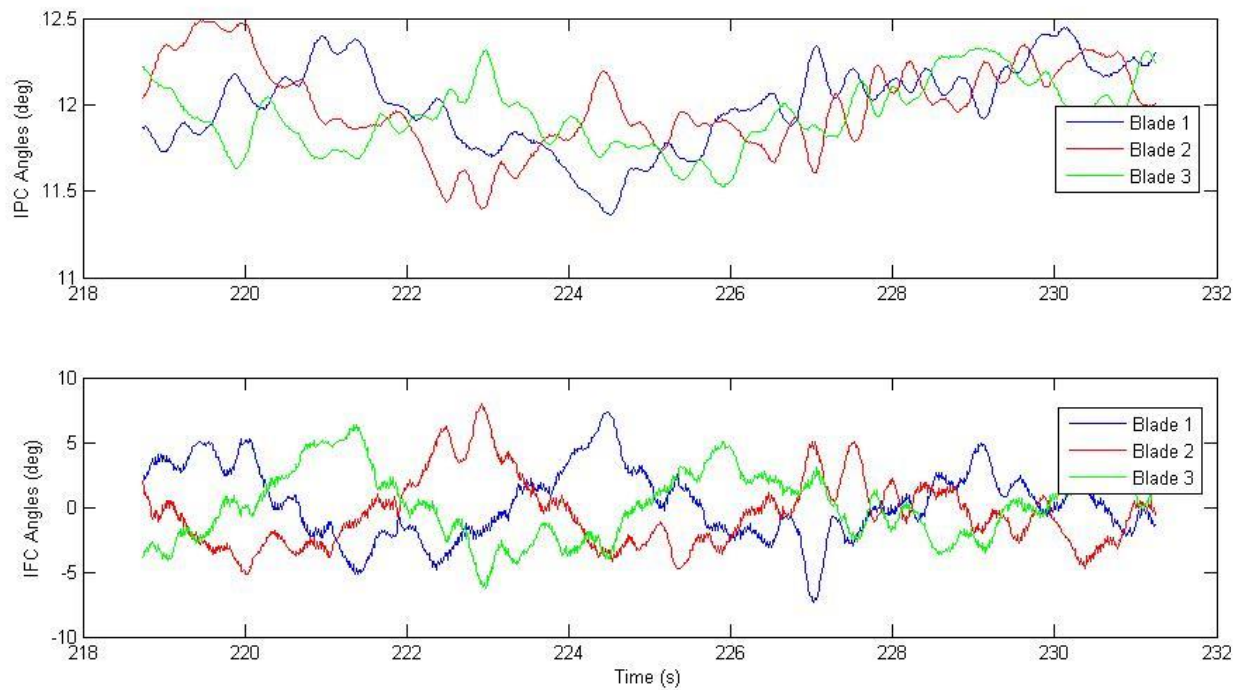


Figure 4.4: IPC and IFC commands for each blade in above rated conditions

Additionally, the HYBRID controller also shows a reduction in the standard deviation of the tower fore-aft bending moment. Reducing the variation of the flapwise root bending moment on the blades reduces the tilting action of the rotor. Intuitively, the wind is attempting to tilt the rotor backwards due to wind shear at the top of the rotor, creating a large bending moment at the top of the tower. Alleviating the blade loads decreases the tilting action of the rotor and reduces the variation of the tower fore-aft bending moment by about 5%, as seen in the Figure 4.5 below.

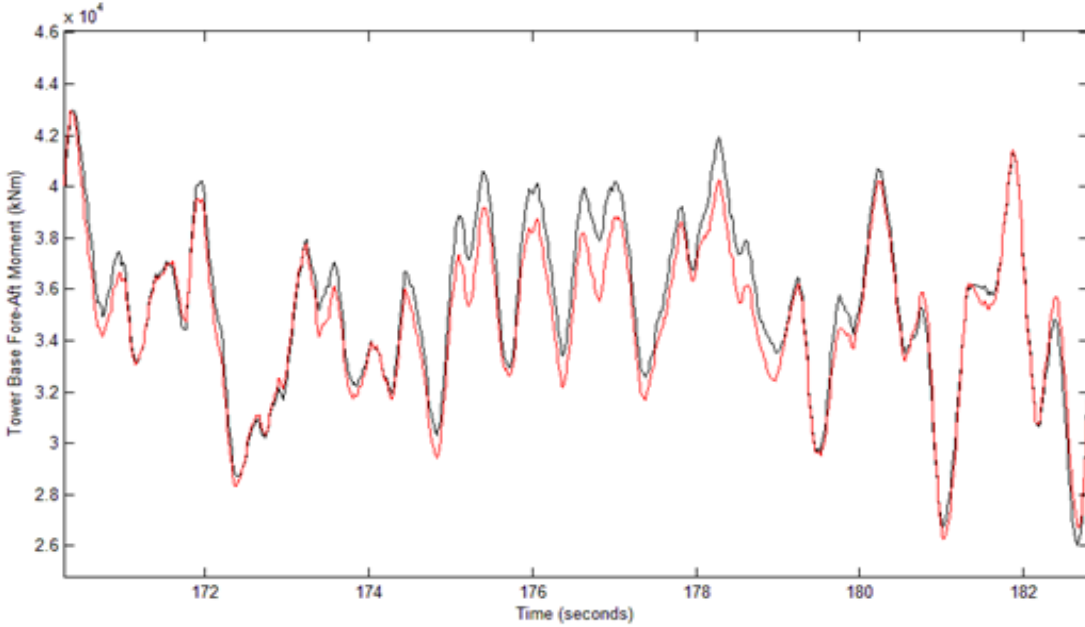


Figure 4.5: Comparison of tower fore-aft bending moment for SC and HYBRID controllers

Any implementation of these controllers would result in improved load reduction and lifespan of wind turbines, which can be seen in Table 4.1. It is also noteworthy that the average root flapwise bending moment is reduced by 1%. The 26.3% reduction in the standard deviation of M_y proves the superiority of this HYBRID control approach.

Table 4.1: Load reduction potential for IFC, IPC and HYBRID controllers for above rated conditions

	IFC % Reduction	IPC % Reduction	Hybrid % Reduction
Moment Average	-1.01	-1.05	-1.08
Moment STD	-13.60	-19.1	-26.30

4.2 Power Loss

As expected, the presence of the TEFs affects the power output in Region 2. Just as the blade pitch is held constant in Region 2 for optimum operation, having a flap deflection of zero is also necessary for maximum power output. Deflecting the TEFs in any direction results in a decrease of the lift to drag ratio, causing power output to also decrease. Figure 4.6 shows the decrease in generator power and rotor speed in Region 2 for the 15% turbulent wind case. Although the average power loss is only about 1.5%, over the turbine's lifespan it will result in a significant loss of revenue.

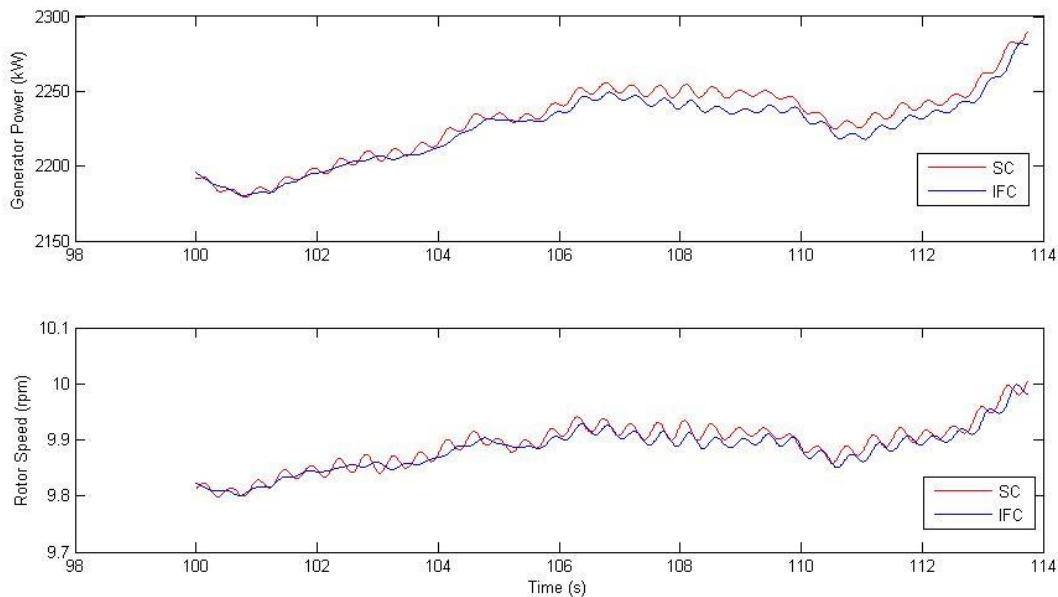


Figure 4.6: Reduction in generator power and rotor speed due to the addition of IFC controller in Region 2

To quantify the impact of the IFC controller on power output, the change in magnitude of the Coleman angle is used for analysis. The Coleman angle represents the collective magnitude of

the flap deflection before it is transformed into each blade individually. A low value of Coleman angle results in small TEF deflections, while high values result in large deflection angles.

Shown below are the results of simulations with a steady 8.5 m/s wind speed, in order to quantify the effects on power, rotor speed and generator torque in the simplest case. A ramp function is used for the Coleman angle input, as opposed to letting the system react to the root flapwise bending moment. Although M_y is replaced with a ramp function, the analysis still holds because the rotor azimuth angle ψ inputted into the Coleman matrix keeps the flap deflection signal in phase with the outputs.

The Coleman angle is ramped from 0 to -0.17 in order to quantify the effect of the IFC controllers. Figure 4.7 shows that power, torque, and rotor speed decreases linearly with the increase in magnitude of the Coleman angle, as expected. The results of attempting to overcome the power loss due to load alleviation are examined in the following sections.

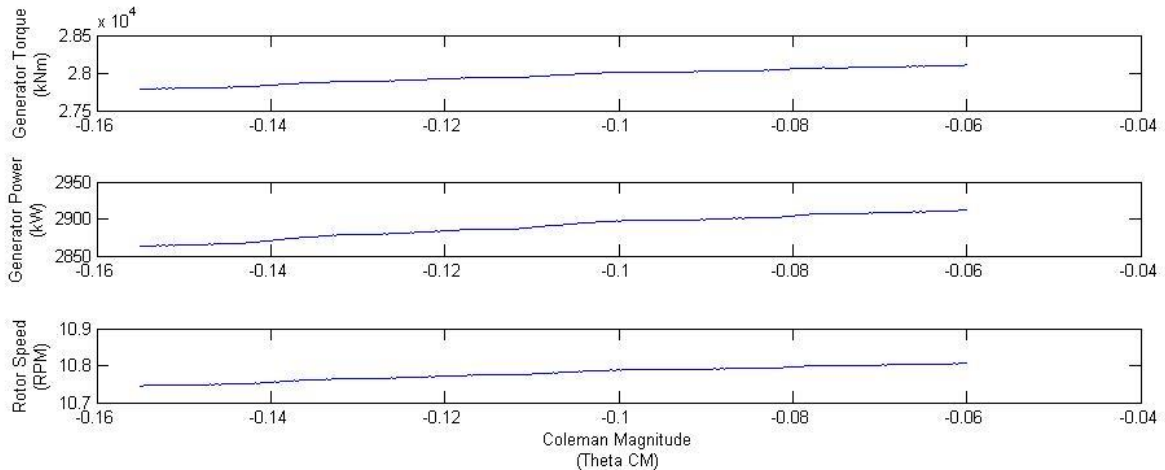


Figure 4.7: Response of torque, power and rotor speed with ramping Coleman angle from minimum to maximum

4.3 Advanced Generator Control Results

The advanced generator torque controllers are applied to the wind turbine model to examine the potential power increase in Region 2. From the results in previous section, a power loss of 1.5% occurs due to the application of the IFC controller. The IFC controller is activated in all simulations so that the advanced generator torque controllers can be evaluated on their ability to increase Region 2 power capture in the presence of a load reduction IFC controller. The generator torque controllers are compared to the IFC cases that use the standard generator torque control (SC) that results in power loss, relative to the baseline control. It should be noted that in this section SC designates the baseline generator control, with the IFC operating as well.

4.3.1 Generator Torque Gain Reduction Results

Decreasing the generator torque gain results in erratic changes in power output. As shown in Figure 4.8, for steady and low turbulent wind there is no advantage in decreasing K to increase power capture with the IFC controller present. Turbulence intensities of 5% and 10% are omitted from the figures and analysis, as there is almost no difference in power production between those turbulence intensity values and the steady wind case. This is mainly attributed to the generator torque not having to adjust to significant gusts and lulls from wind turbulence [5].

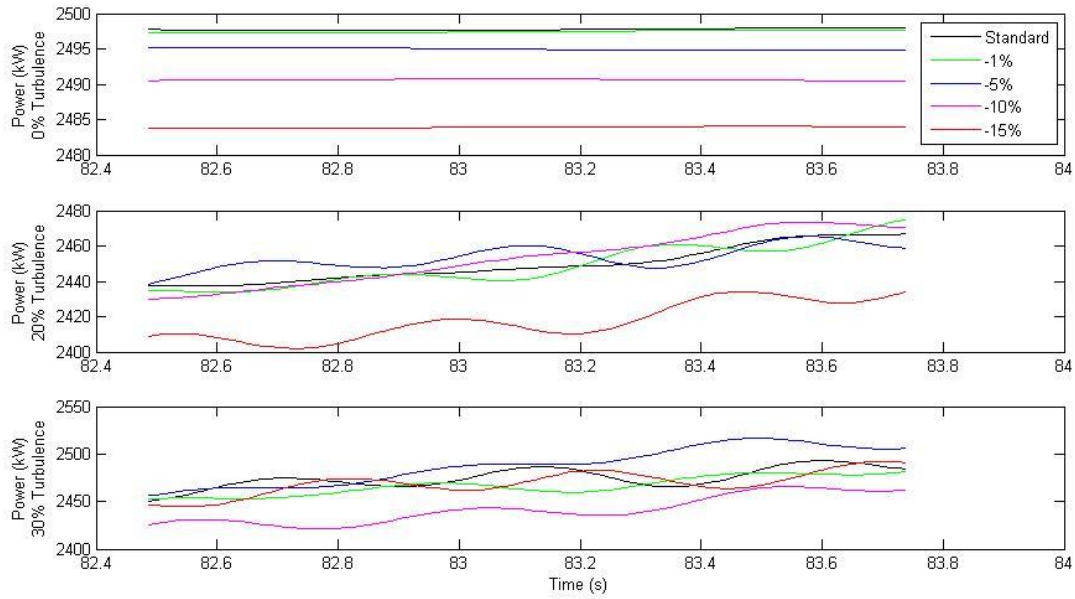


Figure 4.8: Change in power output with K reduction for turbulence intensities of 0%, 20% and 30%

However, for the high turbulence cases, the results show some potential in increased power capture, but not as much as expected. The simulations for turbulence intensity of 20% and 30% are compared through the same time window, but the power output is fairly unpredictable. As shown in Tables 4.2 and 4.3, an increase in the average power capture occurs for high turbulence simulation with a decrease of K between 5% and 10%.

Two causes can easily be attributed to the gain reduction causing different results for each case. The first is the fast fluctuations in wind speed due to the turbulence. Because there is no way for the turbine to quantify the amount of turbulence in the wind, it cannot adjust K fast enough for its optimal tip speed ratio. Calculating K as a function of turbulence intensity could be a more efficient alternative, but as stated, turbulence is difficult to quantify due to its unpredictability.

Additionally, with the IFC controller deflecting each blade separately, measuring the impact on

the rotor collectively adds extra complexity to the rotor dynamics. Essentially, the controller reacts to the loads caused by the fluctuations in wind speed, so it is influenced by the turbulence in the wind. Variations in the turbulence intensity directly affect the rate and magnitude of the flap angles. This adds more fluctuations to the tip speed ratio that make the calculated K value increasingly suboptimal.

Table 4.2: Average power output results in kilowatts for simulations while varying gain reduction and turbulence intensity

Power (kW)	Percent K Reduction				
	Turbulence Intensity	0%	1%	5%	10%
0%	2498.4	2498	2495.5	2491.1	2488.4
10%	2307.8	2307.3	2306	2299.4	2302.6
20%	2158.1	2157.4	2165.7	2166.4	2165.1
30%	2069.7	2065.8	2095.2	2085.3	2085.4

Table 4.3: Percent change in average power output results for simulations while varying gain reduction and turbulence intensity, with optimums highlighted for each case

Turbulence Intensity	Percent K Reduction				
	0%	1%	5%	10%	15%
0%	0.00	-0.02	-0.12	-0.29	-0.40
10%	0.00	-0.02	-0.08	-0.36	-0.23
20%	0.00	-0.03	0.35	0.38	0.32
30%	0.00	-0.19	1.23	0.75	0.76

4.3.2 Wind Speed Standard Deviation Torque Controller Results

The inputs for this controller are varied over a range of bin sizes and turbulence intensities to test its efficiency. By observing the wind data from the 80 Hz FAST simulation, the variations between each time step are minimal, so a sampling rate of 1 Hz is utilized. Using the 1 Hz input

to the controller commands it to take the average of the wind speeds over a one second period. The variation of the averages between one second period is significant enough to demonstrate the variations in the wind.

The bin size for the standard deviations are varied between 10, 15, 25, and 50 seconds in order to quantify the turbulence in the wind. This range is used so that the effect of the magnitude of the variance on the controller can be easily observed. Intuitively, having larger bin sizes reduces the effect of sudden gusts in the wind because of the larger sample. The gain of the controller is directly proportional to the magnitude of the standard deviation of the bin size and adjusts the generator torque accordingly.

Just as in the previous section, the same wind files with turbulence intensities of 10%, 20% and 30% are used in order to compare the power production results of this control approach to the simplified gain reduction scenario. Overall, the results of the controller are successful, which are reflected in the tables and Figures 4.9 and 4.11 below.

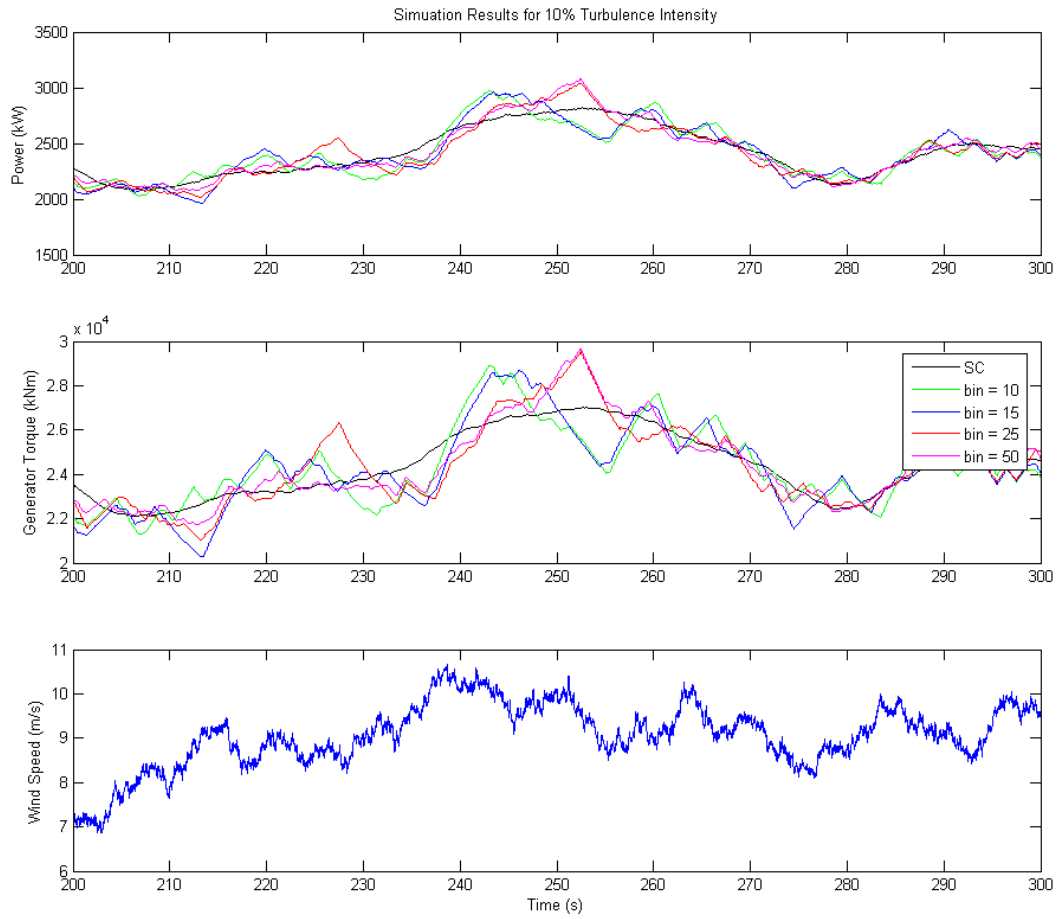


Figure 4.9: Simulation results for wind file with 10% turbulence intensity

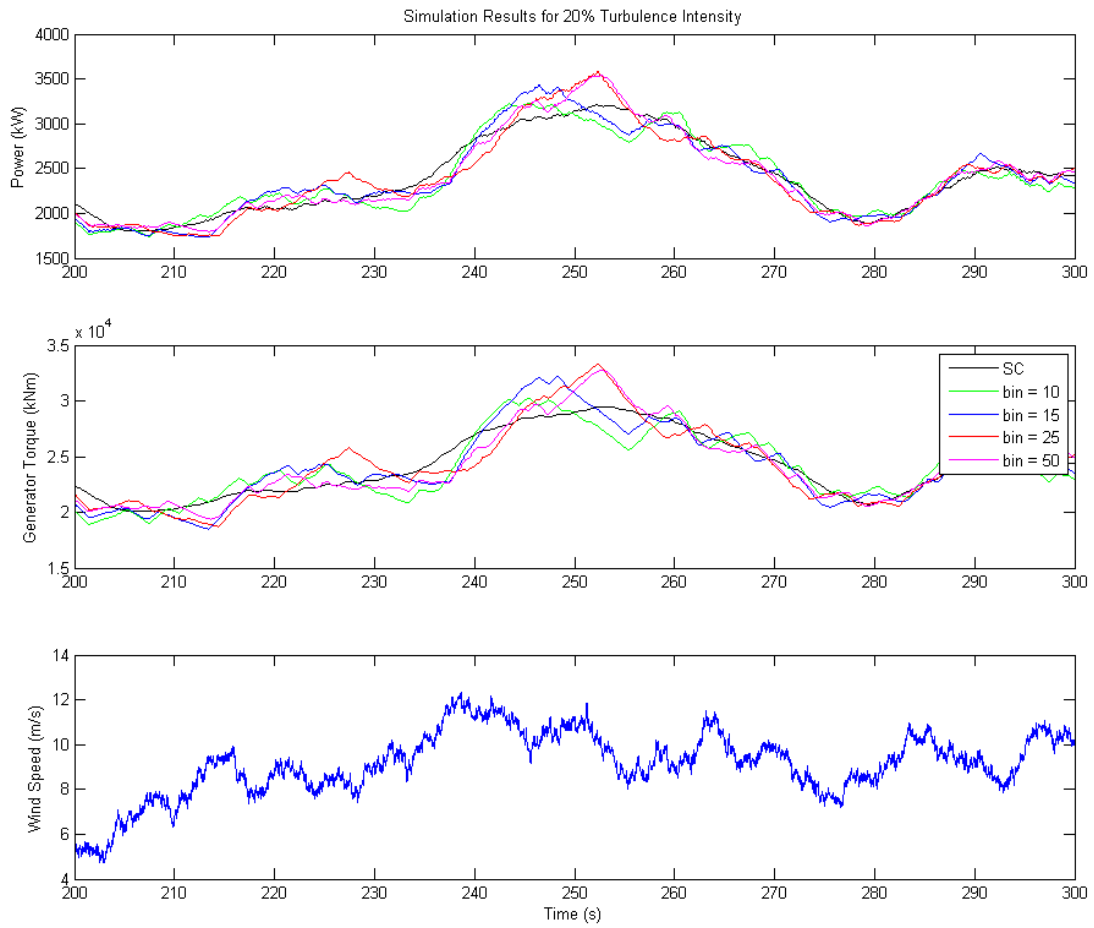


Figure 4.10: Simulation results for wind file with 20% turbulence intensity

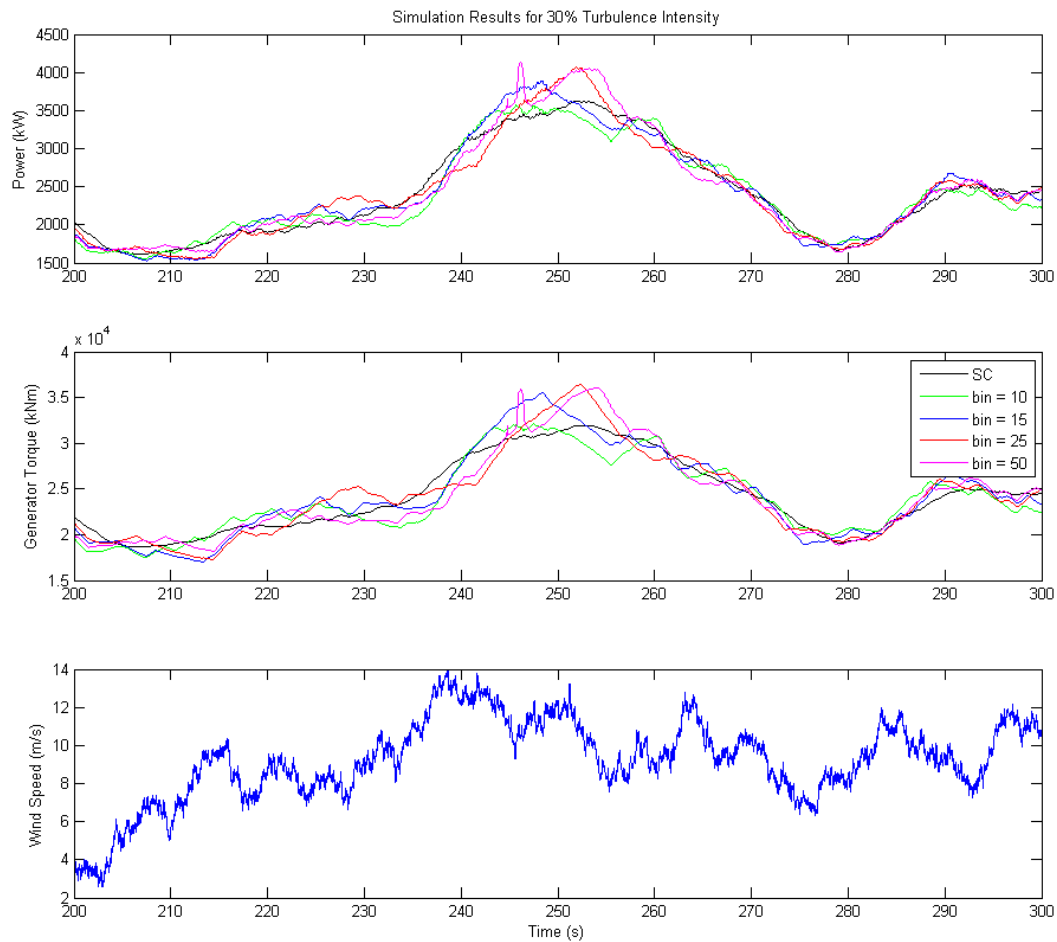


Figure 4.11: Simulation results for wind file with 30% turbulence intensity

Unlike the results from Table 4.3, all the simulations performed for the wind speed STD Controller result in increases of the average power. By observing the wind speeds from the simulation, the greatest power increases occurs during the gusts and lulls of the wind. Specifically, at the time step of 238 seconds, a large increase in wind speed occurs, during which the generator torque drops significantly compared to the standard control case. What follows is a large spike in power output once the wind speed begins to settle. During periods where the wind speed is fairly

steady, there is not much variance in the generator torque, which results in a normal amount of power being produced. There are differences in the power production with the different bin sizes that are tested, which can be seen in Tables 4.4 and 4.5 below.

Table 4.4: Power output for wind STD Controller

Power (kW)	Bin Size (s)				
Turbulence Intensity	SC	10	15	25	50
10%	2537	2551	2544	2539	2555
20%	2639	2656	2641	2640	2656
30%	2750	2756	2771	2748	2784

Table 4.5: Percent power difference for wind STD Controller

Percent Difference	Bin Size (s)			
Turbulence Intensity	10	15	25	50
10%	0.552	0.276	0.079	0.709
20%	0.644	0.076	0.038	0.644
30%	0.218	0.764	-0.073	1.236

From the simulation results, the maximum power increases occur for the bin size of 50 for the 10% and 30% turbulence intensities. The 20% turbulence case shares the same power increase for bin sizes of 10 and 50 s. A situation that could explain this result is a wind sample that has a significant difference between the wind speeds at its tail ends. For example, the wind speeds for a bin can have fairly steady wind throughout its record, but also have an extreme gust and lull at its beginning and end. This would cause a large increase in standard deviation of the sample, which would result in a less than ideal gain variation for the turbine.

Although these cases may exist and cannot be predicted, overall the controller is successful in increasing the power production in almost every simulation of varying bin size and turbulence intensity. It seems that the general bin size of 50 s gives the most consistent results and could be

used in future controllers. It is also important to note that the accuracy of the measurement of the wind speed magnitude is not important, as long as the variability of the wind is measured.

4.3.3 Tip Speed Ratio Tracking Controller Results

The TSR tracking control method proves to have favorable results compared to the standard generator control, as shown in Figure 4.12 where IFC is activated in both cases. It is easily observed that the variance of the generator torque command has decreased. This is attributed to the controller changing the rotor inertia to operate towards the set point of $\lambda = 7.55$, its design optimum. Although the standard generator gain is calculated to accelerate the rotor towards its optimal tip speed ratio, the tracking method allows it to speed up the action. The simulations reveal an average power improvement of 1.07%, which is significant compared to the 1.5% power loss of the baseline case due to the IFC.

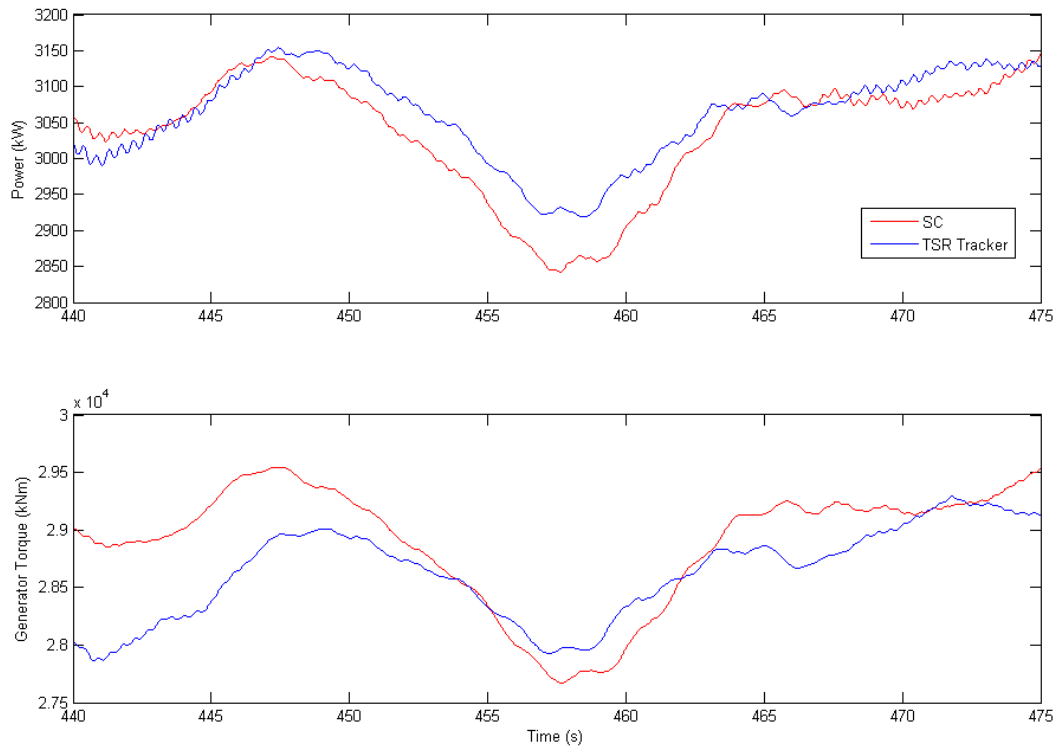


Figure 4.12: Power output and generator torque commands from TSR tracking controller with IFC activated

4.3.4 Power Production Results with Wind Speed Estimation Error

The introduction of wind speed error has negative effects on the power output as expected. The addition of the error to the TSR tracking controller causes the range of the generator torque to increase, which is reflected in Figure 4.14. Although the controller adjusts the gain so that it accelerates towards its set point, the magnitude of the gain is inaccurate due to the tip speed ratio input being altered by the wind speed error.

Referring to the 1% case and 20% case specifically, the ranges of the generator torque for these cases are much larger; but when comparing the power outputs in Figure 4.14, the difference in power output seems minimal. Having error in both the positive and negative direction has almost identical consequences on the power, which proves that any error in knowledge of the turbines true tip speed ratio has adverse effects on its performance.

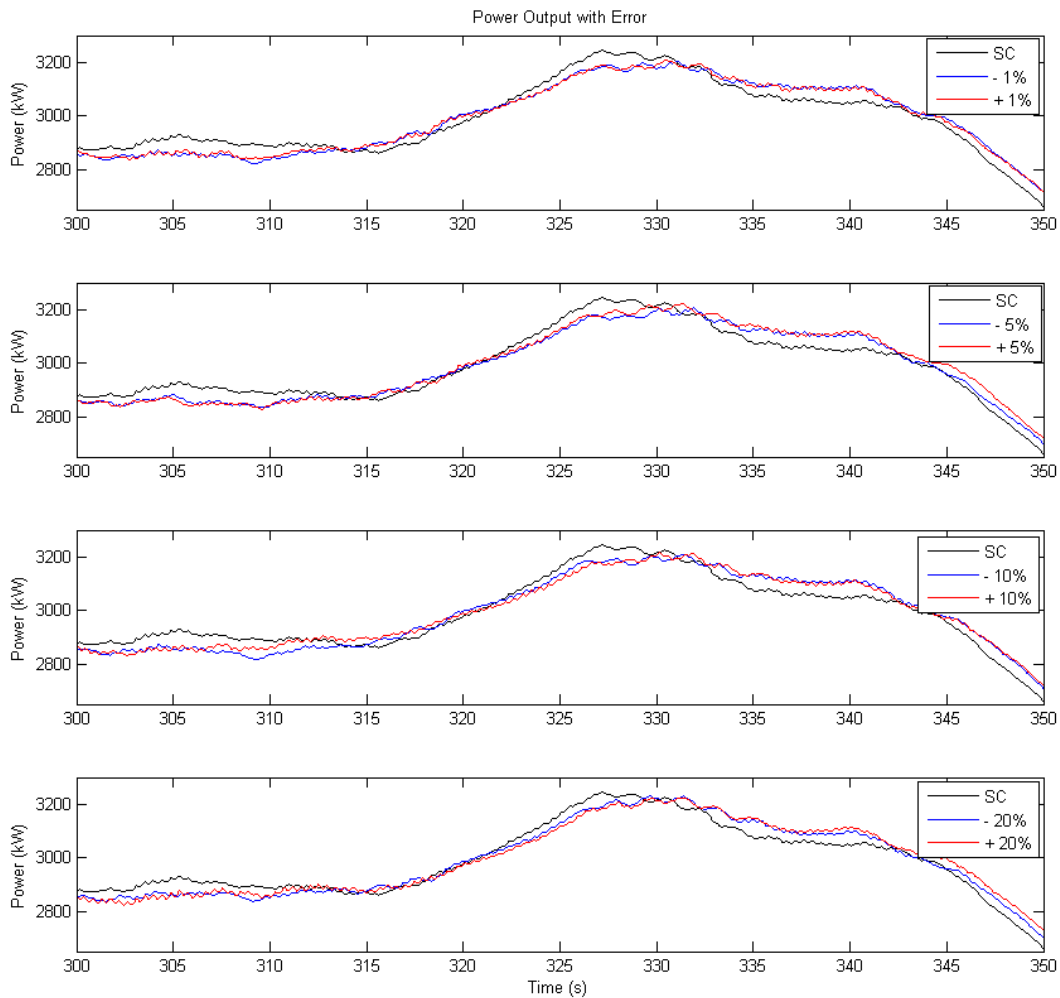


Figure 4.13: Power output with wind speed error introduced to TSR tracking controller

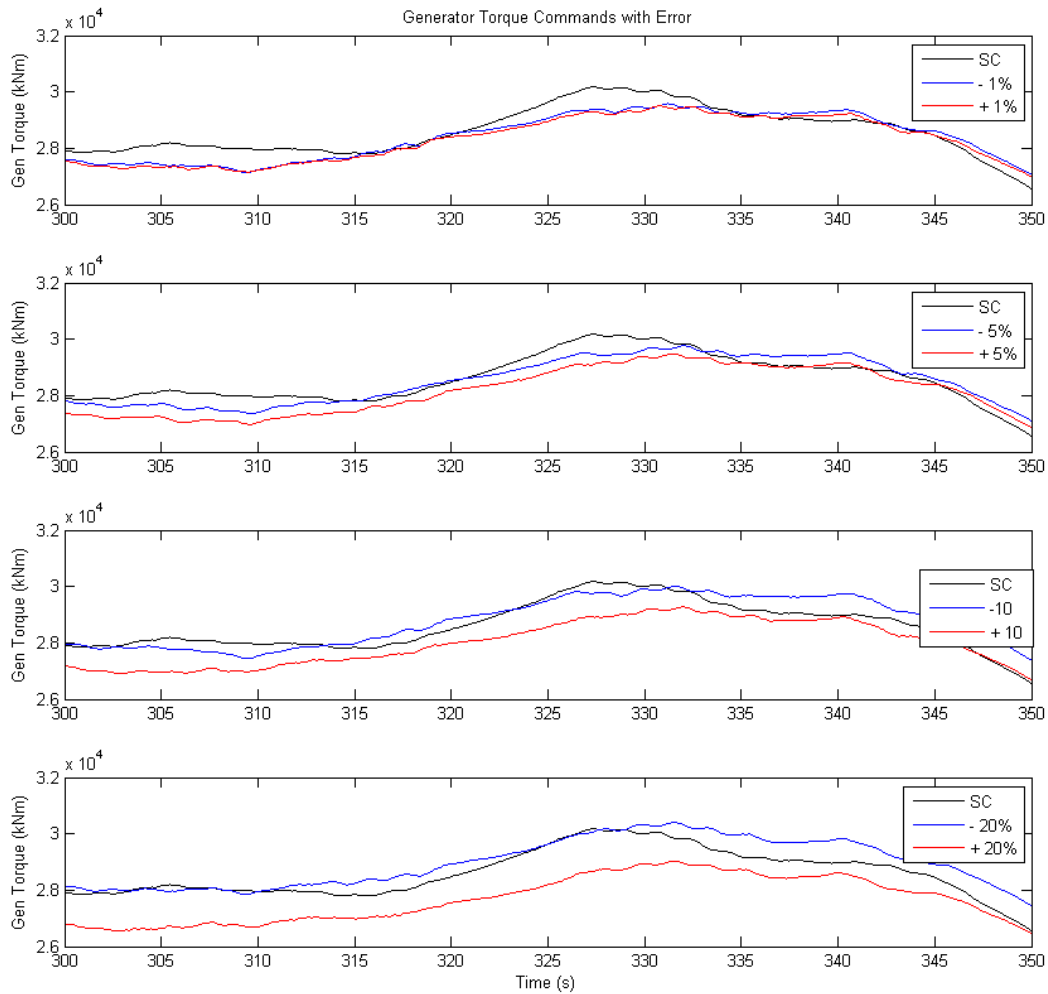


Figure 4.14: Generator torque commands with wind speed error introduced to TSR tracking controller

However, it is worth examining the trend of the power loss from the wind speed error. One may assume that the increase of error would also cause the power production to decrease. The comparison of power reduction in Table 4.6 indicates a fairly constant decrease in power no matter how large the error in wind speed. The controller is sensitive to any uncertainties, and introducing

wind speed error into the controller negates its control approach. Thus, the control algorithm is not very robust to measurement error. As of now it is unclear as to what causes this unexpected scenario, but it leads one to believe that the TSR control algorithm can further be refined.

Table 4.6: Percent power loss for various error estimates

Percent Error (+/-)	Percent Power Loss
1	0.97
5	0.96
10	0.83
20	1.1

4.3.5 Smart Rotor Torque Regulation Results

The control algorithm for the SRTR yields less favorable results for increasing Region 2 power capture, compared to the TSR tracking controller. The tip speed ratio error tracking term $K\lambda$ allows the rotor to accelerate and decelerate to more optimum values that correspond to its design tip speed ratio, making the Region 2 operating conditions more ideal. Additionally, the $K_{CM}(\theta^{cm_3})$ term conserves the momentum of the rotor rotation according to flap angle, resulting in an increase in rotor speed of about 1.5%, while increasing the power by 0.05%. The turbulent wind does cause issues for the controller however, since the wind speed fluctuates significantly with each time step causing an erratic change in tip speed ratio, as well as the Coleman angle. To overcome this rapid fluctuation, a low pass filter is implemented to smooth the signal and cause less fluctuations for the rotor to adjust to. Figure 4.15 displays the new generator torque command and its effect on the power output.

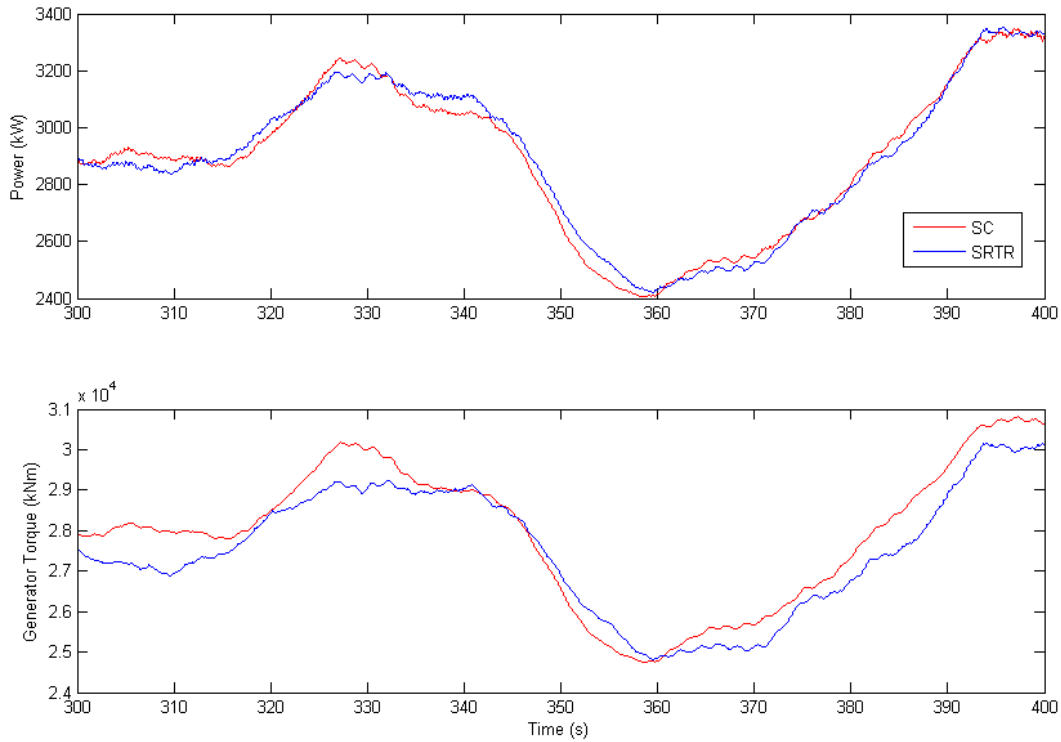


Figure 4.15: New generator torque commands and power output for SRTR controller

A total power increase of 0.85 % over the 400 second simulation is achieved in comparison to the standard generator control (SC). The drop in power capture compared to the TSR tracking controller is due to the addition of the Coleman angle term. The addition of the term adds unnecessary change to the gain, causing a less ideal operating condition.

4.3.6 Recalculating K based on C_P for Varying Flap Deflection Angle

As explained in section 3.2.6, the concept behind this controller is to calculate the exact generator torque gain based on the power coefficient calculated by the varying TEF angles of the

individual turbine blades. Using Figure 2.1, the local C_P for each blade is retrieved and averaged together for the controller to create a collective C_P value. Because this is a real time controller, the power coefficient is calculated at a frequency of 80 Hz, the same as the FAST simulation. The degree of variability of the gains, which is seen in Figure 4.16, is due to the rapid response of the controller to the TEF angle of each blade.

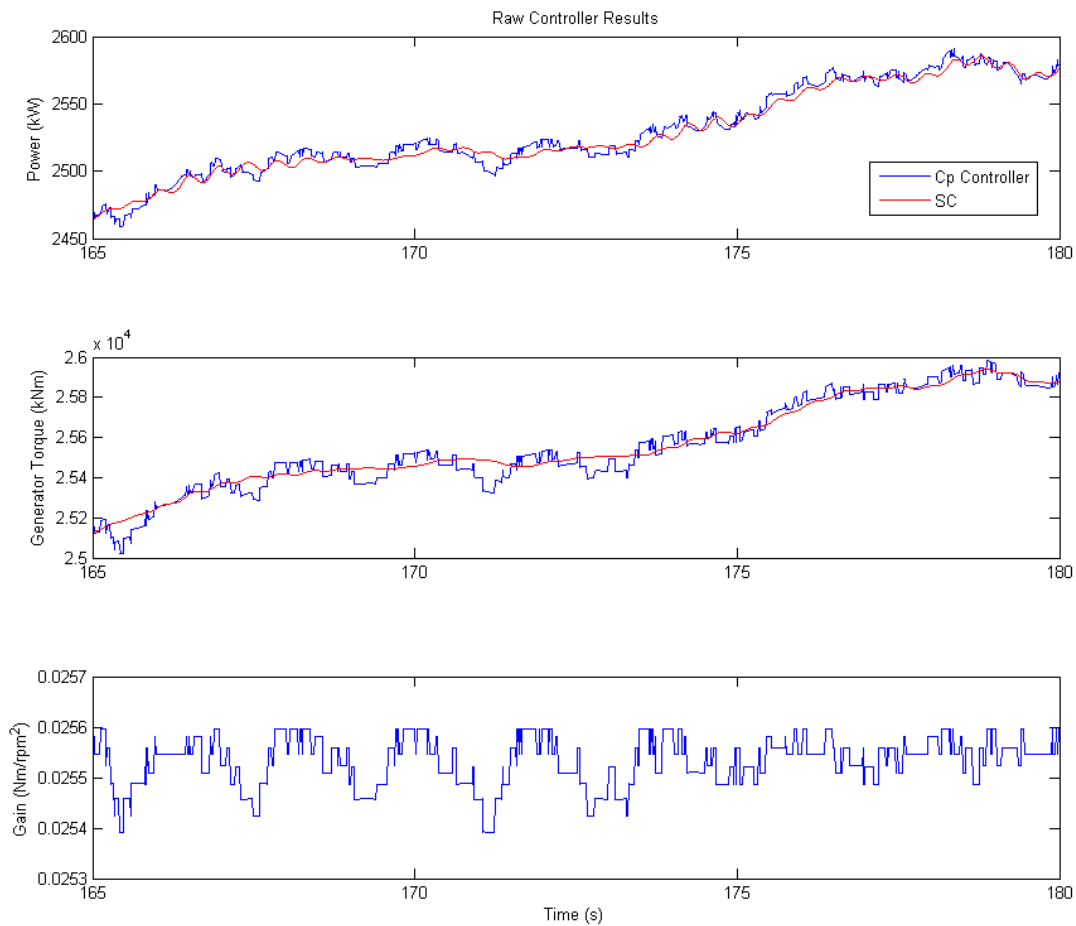


Figure 4.16: Raw controller results for C_P calculation controller

Although this seems like an accurate representation of the turbine's gain variation, in actuality, the turbine cannot react fast enough to the rapid change of the generator torque. The result of this raw signal is a power loss of 0.8%, compared to the standard generator control with IFC active, which leads one to believe that this approach is not plausible.

To overcome the turbine's inability to respond to the rapid gain change, a rate limiter is implemented to make the variations between time steps less erratic. The addition of the rate limiter is successful in filtering the signal, as seen in Figure 4.17.

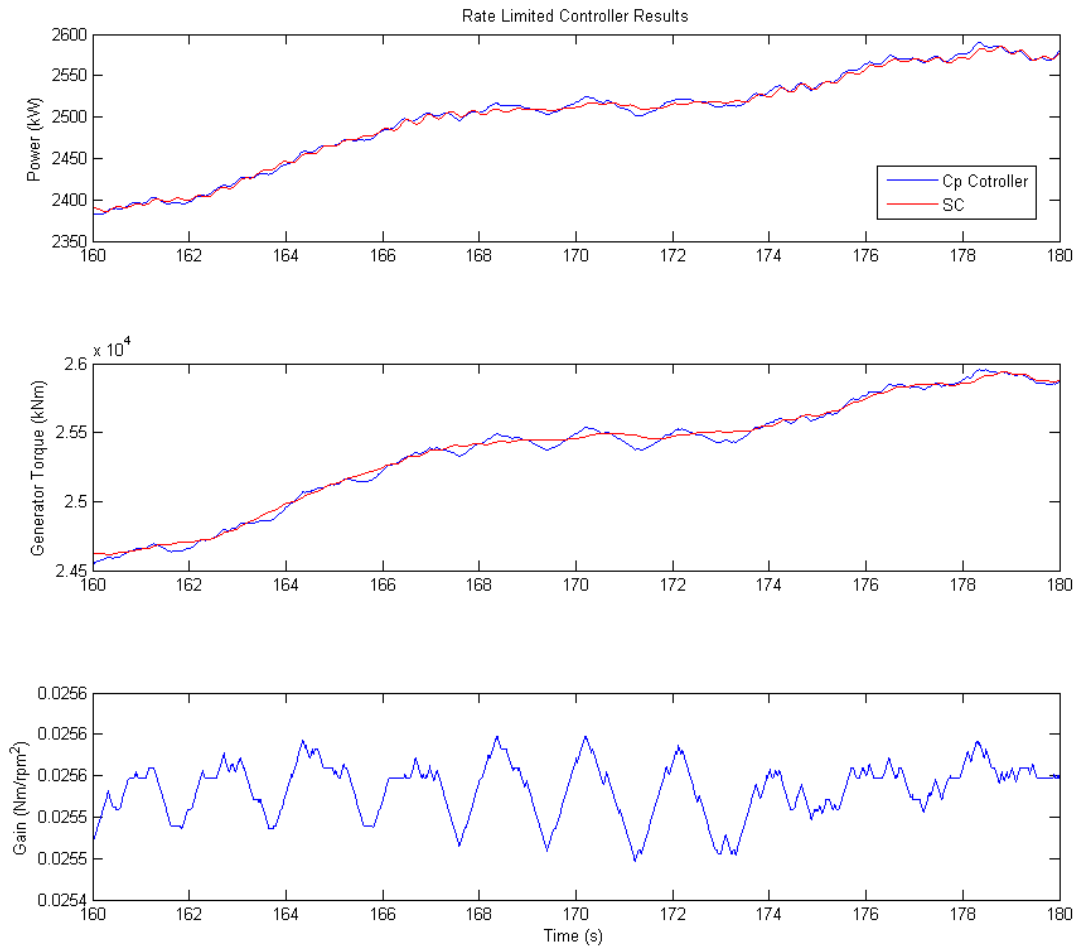


Figure 4.17: Filtered results for C_p calculation controller

Although successful in making the gain variations less erratic, the resulting average power increase from this controller is 0.13%. Because there is currently no validated research to compare, it is unclear as to why this methodology does not produce favorable results. Further research is required to refine the controller and test its efficiency.

4.3.7 Linear Quadratic Regulation Control

The Q and R matrices are chosen to create a gain that results in a small increase in power output. To simulate this, the element of the weighting matrix for power, $Q(2,2)$, is slightly increased by 5% to put an emphasis on the power output of the state space model. The built in LQR function in Matlab creates the optimal gain for these conditions.

To compare the effects that the changing of the weighting matrix has on the system, the default Q is calculated by using the equation below, where C is the controllability matrix of the state space model. This is the simplest case of the weighting matrix, which sets the weights of the state variables equal to each other.

$$Q = C' * C \quad (4.1)$$

Using these Q values, the step response of the system with the LQR controller is simulated and can be seen in Figure 4.18.

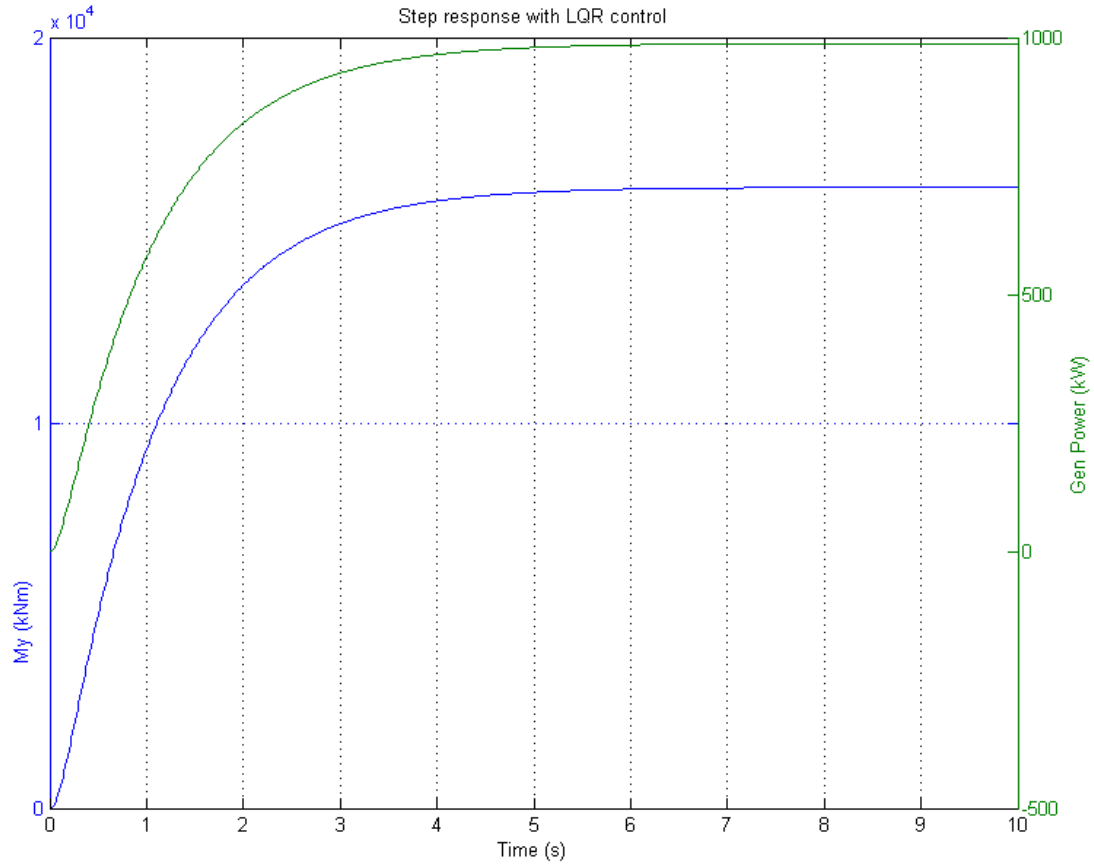


Figure 4.18: Step response of state space model

With a baseline case to compare to, the LQR gains with Q increased for power is simulated and can be seen in Figure 4.19. By increasing the weighting for power, the step response for that output now lies slightly above 1000 kW, while the original case lies just below that value. The assumption made from observing Figure 3.10, that there is strong coupling between the inputs and outputs, seems to stand because increasing the power also increases the value of My^{CM} . The increase seems minimal, but it is proportional to the power output increase from the LQR control with weighted Q .

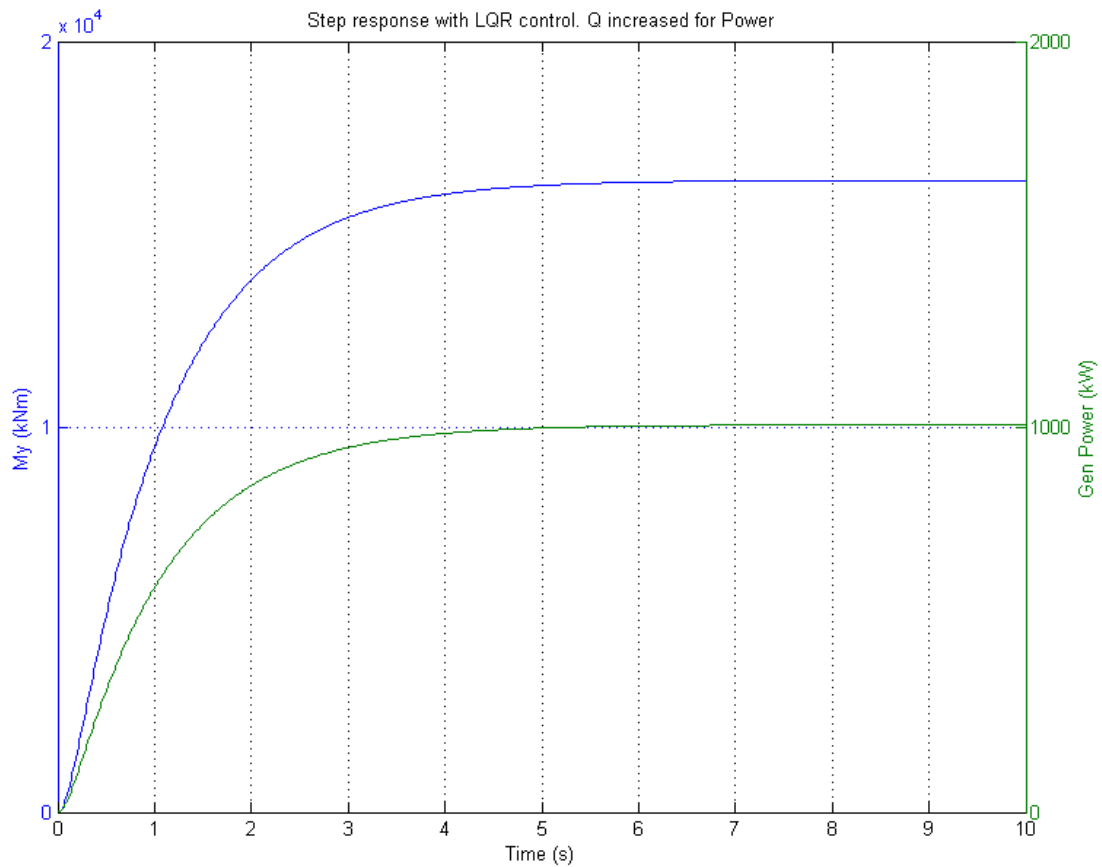


Figure 4.19: Step response with LQR controller for Q increased for power

The issue arises when applying the optimal gain from the LQR controller to the actual model in FAST. The application of this controller causes the simulation to crash within seconds, because the plant inputs cannot process some of the inputs. This is most likely due to oversimplify the state space model of the wind turbine. FAST has a substantial amount of inputs and outputs, most of which are coupled together for its simulations. Basing a state space model on two inputs and two outputs is not sufficient to model the complexities of the turbine model, which is most likely why the simulations fail.

4.4 Overview of Results

An overview of the various controllers implemented to the FAST model is displayed in Figure 4.20. The results in this figure represent the increase in the average power capture in Region 2 with IFC activated for every generator torque controller design in this research. The controllers are able to capture a maximum of 1.3% average power compared to standard generator torque control, while maintaining the 12.1% reduction of loads from the IFC. Although not completely overcoming the power loss deficit, combining them with the load reduction capability of smart rotor blades makes it a much more favorable mode of operation. Overall, the results verify that these advanced control approaches are superior to the standard control law for generators.

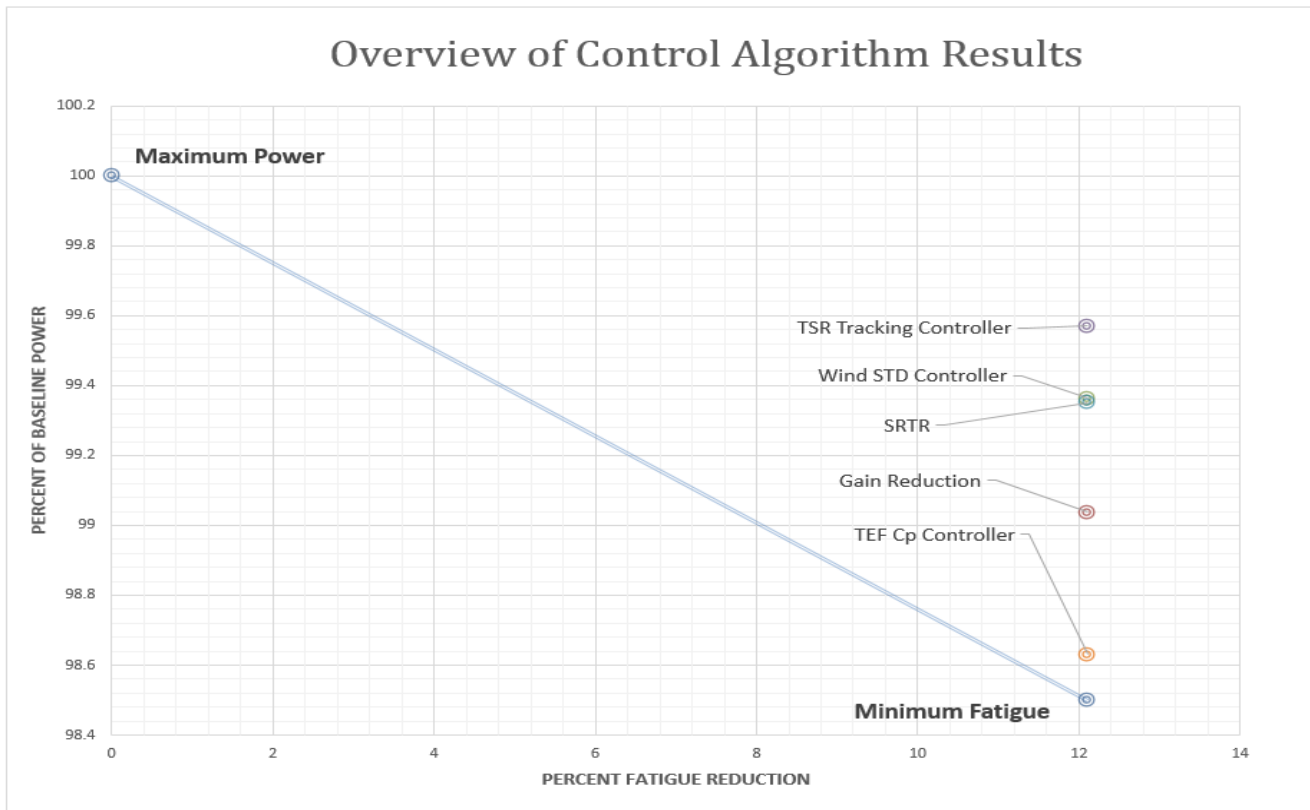


Figure 4.20: Overview of Control Algorithm Results

CHAPTER 5

CONCLUSIONS

This research explores the load reduction and power capture increase of the NREL 5 MW from the various control algorithms implemented. The addition of smart rotor control to wind turbines is shown to significantly decrease unsteady blade loading. While these controllers greatly decrease rotor fatigue, the consequence on power loss from manipulating the turbine aerodynamics are non-negligible. Thus the research goal is to overcome this loss in power through generator torque control. The advanced generator torque controllers are successful in improving the power capture, while maintaining the load alleviation capabilities of smart rotor controllers.

While gaining approximately 1-2% of power production seems minor, coupling this with the increase in lifespan from the smart rotor controllers, the revenue increase is significant. The main conclusions in this research are:

- The smart rotor control designs implemented into FAST prove to be a potential solution to rotor fatigue and reduced maintenance cost for multi-megawatt wind turbines. Whether IPC, IFC, or HYBRID controllers are utilized, they are superior to standard control in their ability to reduce the loads that blades are subjected to.
- In above rated conditions, the IPC controller results in greater load reduction compared to the IFC controller. This is because pitching the blade has an effect on every one of the blades segments, while deflecting the flaps only change the aerodynamics of the outer 70-90% of the blade. However, the HYBRID control approach of the combined IPC and IFC controllers garners the greatest load reductions, decreasing the flapwise root bending moment standard deviation by 26.3%.

- Although the addition of the IFC controller reduces the standard deviation of the loads by 12.1% in below rated conditions, this results in an average power loss of about 1.5%. Manipulating the aerodynamics of the blades causes a reduction of the ratio of the coefficients of lift and drag, effectively slowing down the rotor and decreasing power capture. The generator torque gain is no longer optimum because of the change in the aerodynamic properties of the rotor.
- Reducing the value of K shows potential, but only for the high turbulence simulations. The increase of average power capture is about is less than 1% in comparison to the standard K . However, the relationship between gain reduction and turbulence intensity is not as expected.
- The wind speed STD controller is much more successful in capturing power than simply reducing K . Utilizing the deviations in the wind from past data allows the generator to adjust its torque according to the gusts and lulls of the wind. The relationship between wind turbulence intensity and generator gain is found to be inversely proportional, as expected. Overall the larger bin sizes result in the most power improvement from taking wind samples at 1 Hz. Further analysis using varying random seeds for the wind files over the various turbulence intensities yielded consistent simulation results. The controller results in a maximum power increase of 1.24% and averaging an increase of 0.863% over the various turbulence intensities simulated.
- The TSR tracking control method is the most successful in improving power performance for the smart bladed turbine. Allowing the turbine to operate closer to its optimal operating point results in more efficient operation. Filtering the signal is integral in the achievement of the power increase because it rejects the fast fluctuations

in tip speed ratio due to turbulence, and gives the rotor more time to react to the torque change. The power increase of 1.07% nearly overcomes the power loss when using IFC, while maintaining the fatigue reduction capabilities.

- The controller designs that are based on wind speed and TSR tracking may have practical limitations because of the difficulties in measuring the wind speed accurately. By introducing error into the TSR tracking controller, its efficacy is tested and the effects of inaccurate wind measurements are noticeable. Any uncertainty that is added to the wind speed results in a loss of average power production. This leads one to believe that controllers relying on accurate measurements of wind speed may not be robust.
- The design of the smart rotor torque regulator (SRTR) is successful in slightly increasing power capture in Region 2. However, the gain that corresponds to the Coleman angle causes the controller to compete against the TSR gain. It does result in a smaller power increase of 0.85%, which makes the addition of the Coleman angle negligible.
- The real time calculation of K based on the TEF angles is not as successful as expected. Conceptually, the algorithm seems promising, but the variations of C_P are too erratic for the turbine to react to. Although the addition of the rate limiter greatly decreases this, it results in a power increase of only 0.13%.
- From the initial testing of the LQR model, the increase in the weighting of the power results in the increase of My^{CM} for the simplified state space model estimated for the turbine. However, the LQR controller gains are not applicable to the FAST model; its implementation causes the simulation to crash almost immediately. This leads one to

believe that increasing the power output is much more complicated of a problem than expected. Using a simplified state space model is not an accurate representation of the complexities of FAST.

CHAPTER 6

FUTURE WORK

The control designs and simulation results are explored throughout this research and show promise in both decreasing rotor fatigue and increasing energy capture. The smart rotor control algorithms for this model show similar results to control designs that are implemented in previous research in the attempt to alleviate blade loads [1] [3] [6]. Furthermore, the various algorithms that are designed to control generator torque to improve power capture are successful. Although they do not completely overcome the power deficit that results from the load alleviation of the IFC, they produce a significant amount of power that supplement the loss. The results and analysis from the simulations reveal that further tuning and examination needs to be done to improve the performance of the less successful controllers.

6.1 Smart Rotor Torque Regulator Control Refinement

The design for the SRTR is capable of improving power capture by about 0.85% in Region 2. The generator torque gain is mainly dictated by the tip speed ratio error by using a set point of 7.55, the design optimum tip speed ratio for the NREL 5 MW wind turbine. The concept behind adding the Coleman term is to help conserve rotor speed from knowing the turbines blade position. However, the addition of the Coleman angle for gain adjustment causes a lower overall power production in comparison to the TSR tracker. Adjusting the gain that corresponds to the Coleman angle does not cause the power output to exceed 0.85%.

From Figure 4.7, the relationship between power output and the Coleman angle is inversely proportional. Logically, an increase in power performance is achieved by decreasing the magnitude of the Coleman angle, which causes a smaller variation in TEF angle. However, this approach is counter-intuitive to the goal of maintaining the fatigue reduction capabilities of the smart bladed rotor while improving power capture. Additional research must be done to examine the effect that the Coleman angle has on other outputs of the rotor.

6.2 Real Time K Calculations Based on TEF Deflection Angles

The results for the real time K calculator do not yield power capture improvement as desired. The signal noise from re-calculating the gain for small time steps does not improve the power, even though conceptually it seems like an accurate modeling procedure for the varying TEF angles. Although the addition of the rate limiter is successful in significantly filtering the erratic gain signal, it is only able to improve the power production by 0.13%.

An alternative addition to the controller that may improve the production is varying its calculation frequency. The current controller design computes a gain at every step of the simulation, which is at a frequency 80 Hz. By decreasing the calculation frequency of the controller, less significant transitions between data points are attainable, giving the rotor more time to adjust to the gain. This strategy coupled with rate limiting might be a promising solution if it is explored further.

6.3 Offshore Analysis

This research is focused on the load reduction capabilities of smart rotor control for onshore wind turbines. Referring to Figure 4.5, the reduction in the tilting moment of the rotor from both the IPC and IFC causes a reduction in the tower fore-aft bending moment. The effect of the decrease in the tilting moment of the rotor is worth exploring for offshore wind turbines.

Offshore turbines with monopile foundations have hub heights comparable to that of onshore turbines, but the tower structure has a much greater length depending on the depth of the water. This extended tower height causes much larger base bending moments, which are harmful for the structure. Although the water provides for some damping of the structure, the motions of the wind turbine are still significant due to the size of the tower.

Structural control of offshore wind turbines is a heavily researched area, due to the abundance of steady wind resource over bodies of water. Lackner et al. has investigated the effects of tuned mass dampers (TMD) on offshore wind turbines to reduce loads and improve structural response. [7] The result of this control approach is a significant decrease in the fatigue loads, as well as the fore-aft motion of the structure. The addition of smart rotor blades has proved to reduce loads on the tower for-aft moment. Coupling these two control techniques may further reduce fatigue loading on offshore wind turbines and minimize the need for maintenance.

BIBLIOGRAPHY

- [1] Andersen, P.B., 2005. Load alleviation on wind turbine blades using variable airfoil geometry (2D and 3D study). *Technical University of Denmark*.
- [2] Balas, M.J. & Pao, L.Y., 2004. Methods for increasing region 2 power capture on a variable-speed wind turbine.
- [3] Bossanyi, E., 2003. Individual blade pitch control for load reduction. *Wind energy*, 6(2), pp.119–128.
- [4] Jonkman, J.M. et al., 2009. *Definition of a 5-MW reference wind turbine for offshore system development*, National Renewable Energy Laboratory Colorado.
- [5] Johnson, K.E., 2004. Adaptive Torque Control of Variable Speed Wind Turbines. *National Renewable Energy Laboratory*.
- [6] Lackner, M., 2009. An Investigation of Trailing Edge Flaps in a Wind Turbine.
- [7] Lackner, M.A., and Rotea, M.A. Passive structural control of offshore wind turbines. *Wind Energy* (September 2010). DOI: 10.1002/we.426

- [8] Laks, J.H., Pao, L.Y. & Wright, A.D., 2009. Control of wind turbines: Past, present, and future. In *American Control Conference, 2009. ACC'09*. pp. 2096–2103.
- [9] Pierce, K., 1999. Control Method for Improved Energy Capture Below Rated Power (Preprint prepared for ASME/JSME).
- [10] Stol, K.A., 2003. Disturbance tracking control and blade load mitigation for variable-speed wind turbines. *TRANSACTIONS-AMERICAN SOCIETY OF MECHANICAL ENGINEERS JOURNAL OF SOLAR ENERGY ENGINEERING*, 125(4), pp.396–401.